THE MECHANISMS OF RIBOSOME RESCUE IN BACILLUS SUBTILIS

by

Esther Nayoung Park

A dissertation submitted to Johns Hopkins University in conformity with the

requirements for the degree of Doctor of Philosophy

Baltimore, Maryland
March 2024

Abstract

Stalled ribosomes are rescued by pathways that recycle the ribosome and target the nascent polypeptide for degradation. In *E. coli*, these pathways are triggered by ribosome collisions through the recruitment of SmrB, a nuclease that cleaves the mRNA. In *B. subtilis*, the related protein MutS2 was recently implicated in ribosome rescue. Here we show that MutS2 is recruited to collisions by its SMR and KOW domains, and we reveal the interaction of these domains with collided ribosomes by cryo-EM. Using a combination of *in vivo* and *in vitro* approaches, we show that MutS2 uses its ABC ATPase activity to split ribosomes, targeting the nascent peptide for degradation through the ribosome quality control pathway. However, unlike SmrB, which cleaves mRNA in *E. coli*, we see no evidence that MutS2 mediates mRNA cleavage or promotes ribosome rescue by tmRNA. These findings clarify the biochemical and cellular roles of MutS2 in ribosome rescue in *B. subtilis* and raise questions about how these pathways function differently in diverse bacteria.

Primary Reader and Advisor: Rachel Green Ph.D.

Secondary Reader: Stephen Fried Ph.D.

Acknowledgements

I am immensely grateful to my advisors, Rachel Green and Allen Buskirk. They have always devoted energy into training not only scientifically and technically but also all of the soft skills needed to be a fully trained scientist. They have always strived to be the best mentor for me and always supported me and cheered me on and fostered a healthy culture in lab.

This Ph.D. was one of most joyful years of my life because of the lovely people in the entire lab. I want to thank Julie Brunelle, who is the most amazing and kindest lab manager in the world. Our science would not be possible without her. I want to thank all of the postdocs: Nicolle Rosa-Mercado, Franny Diehl, Marco Catipovic, Niladri Sinha, Josh Black, Eugene Park, and Chien-I Yang. They have always cared just as much about my work as their own. Without their guidance and ideas, I would have struggled to come out of those scientific lows. I want to also thank all of the other graduate students in the lab: Vienna Huso, Jeff Li, Jake Saba, Miguel Pacheco, and Kate Schole. Coming to lab every day felt like just hanging out with my friends while doing amazing science.

Finally, I want to thank team bacteria: Annie Campbell, Rebekah Berhane, and Kazuki Saito. Kazuki trained me initially in bacterial genetics and without him my technical skills would not be as well trained. Annie and Rebekah have been my rocks throughout this Ph.D. They have been not only been my peers scientifically but also my best friends throughout this journey.

Dedication

This thesis is dedicated to my family: Young Jun Park, Jung Hee Yoon, and Jin Soo Park for not only their unending support and love but also always showing me what perseverance looks like firsthand.

Table of Contents

List of Figures

Chapter 1: Introduction

During elongation, ribosomes sometimes run into problems that inhibit their progression on an mRNA. These stalling events can be short-lived and reversible or long-lived and irreversible. Short-lived pauses can be beneficial to gene expression and protein folding while long-lived ribosome arrest can cause harm to the cell by trapping ribosomes and generating incomplete, truncated proteins.

Programmed pauses can be utilized by bacterial cells to directly regulate gene expression. A key example is the regulation of SecA expression in *E. coli*. SecA is an ATPase that helps proteins translocate through the inner membrane through the SecYEG translocon[1]. SecA expression is regulated by a ribosome stalling event in the gene SecM which located upstream of SecA in the same operon[2]. The nascent chain of SecM interacts with the exit tunnel of the ribosome causing it to stall[3]. When the protein export machinery is working smoothly, the SecM nascent chain is translocated by SecYEG pulling which relieves the stall. When the translocon function is compromised or overwhelmed, however, the ribosome cannot bypass the SecM stall. This affects the folding of the mRNA, opening up the SecA ribosome binding site to allow for translation initiation, and upregulating SecA to increase translocation capability[4]. This ribosome stalling-mediated gene expression regulation mechanism is found in genes encoding protein export machinery in various bacteria such as *B. subtilis* (MifM-YidC2) and *V. cholerae* (VemP-SecDF2) highlighting the importance and utility of programmed ribosome stalling events[5].

Another example of essential and functional stalling is co-translational protein folding. Co-translational protein folding is the process in which a protein folds as it exits out of the ribosome. In fact, this process is often essential for the proper folding of many proteins and prevents misfolding and aggregation[6]. Proteins that require co-translational folding can have regions of low-usage-frequency codons in order to slow down ribosome and allow for the correct protein folding landscape. For example, a circadian clock protein, FRQ, from *Neurospora* utilizes this slow-down of ribosomes. When synonymous mutations are made to more high-usage-frequency codons, FRQ protein had a shorter lifetime and perturbed circadian rhythm *in vivo*[7,8]. This example of programmed stalling shows how finely tuned the rates of translation are.

Unlike programmed pauses, irreversible ribosome arrest is harmful to cells. Irreversible stalls can arise due to chemical damage to the mRNA or antibiotics that prevent elongation[9–11]. Alkylating agents are one example of chemicals that can damage mRNAs. Previous work has shown that alkylating agents cause the accumulation of adducts within RNAs leading to decreased rates of peptide bond formation and irreversibly stall ribosomes *in vivo*[9,10]. Another way to stall ribosomes is through antibiotic treatment. Many antibiotics such as erythromycin and chloramphenicol inhibit bacterial growth by targeting elongating ribosomes, highlighting the toxicity of irreversibly stalling ribosomes and preventing protein synthesis[11].

There is clear evidence that cells utilize ribosome stalling in a functional way, but this stalling can become harmful and unproductive if long lived. So, the question that arises is how do cells distinguish paused and arrested ribosomes? If cells were to target

any stalled ribosome as problematic, productive protein synthesis would be rare. Therefore, differentiating a problematic stall from a productive stall is essential to the viability of cells. Work from both bacteria and eukaryotes has shown that the cell has adapted mechanisms to differentiate the different stalls and rescue the irreversibly stalled ribosomes.

1.1 Rescue of ribosomes stalled on 3' ends

One type of stall is when ribosomes become trapped at the 3' end of messages that lack a stop codon, where the ribosome is unable to recruit release factors. These messages are called nonstop messages and can be generated by various mechanisms. One way is by exo- or endonucleases cleaving the mRNA. Research from Gene-wei Li's group showed that, globally in *E. coli* cells, more than half of the mRNAs are decay intermediates rather than full-length transcripts[12]. If components of the RNA decay machinery are perturbed or inhibited, the number of ribosomes stalled on nonstop transcripts increases, accompanied by an increase in demand for rescue machinery[12]. Another mechanism that generates nonstop mRNAs is premature transcription termination[13]. When transcription terminates early, the transcripts may not contain a stop codon. This is especially a problem in bacteria as translation and transcription occur together. This means that ribosomes have already been loaded on messages that are being transcribed; if transcription terminates early, the ribosomes then stall at the 3' end, emphasizing the need for a mechanism to rescue these ribosomes. Nonstop messages can be harmful to cells not only because they sequester ribosomes but also

because incomplete proteins can cause proteotoxicity. Thus, dedicated rescue pathways are needed to recognize the stalled ribosomes, recycle them, and target the potentially toxic protein for degradation; all of which has been well characterized in bacteria.

1.1.1 Trans-translation rescue pathway

The main pathway in bacteria to rescue ribosomes stalled on the 3' end of messages is called trans-translation. Trans-translation involves a small RNA called tmRNA which, as the name suggests, contains a tRNA-like and an mRNA-like portion. tmRNA is conserved in almost all bacteria, highlighting its essential role for bacterial cell viability[14]. tmRNA is aminoacylated with an alanine residue and is delivered with its protein partner, SmpB, to the ribosomal decoding center by EF-Tu. After peptide bond formation transferring the nascent chain to the alanine on the tmRNA, the ribosome resumes translation on the mRNA portion of tmRNA. When the ribosome encounters the canonical stop codon encoded in the tmRNA open reading frame (ORF), termination and recycling occur as usual[14]. The ORF of tmRNA's mRNA-like portion encodes for a degradation tag (AANDENYALAA) which targets the nascent chain for degradation by the ClpXP protease[15] (Fig 1.1). The two last Ala residues on the degron tag are essential for degradation of the nascent chain by ClpXP; mutating them prevents degradation[16].

One of the most important features of the trans-translation pathway is its specificity for ribosomes stalled on nonstop messages; without this specificity, normal protein synthesis could be affected. The tmRNA/SmpB complex selectively acts on ribosomes stalled on nonstop messages because binding of this complex to ribosomes is

only possible if there is an empty A-site and no downstream mRNA in the tunnel of the ribosome[17]. Structures of the tmRNA/SmpB complex bound to the ribosome revealed that the C-terminal tail of SmpB binds in the mRNA channel of the ribosome[17]. The C-terminal tail of SmpB has many positively charged amino acids and mutations to the tail prevent trans-translation[18]. The structure also clearly showed that tmRNA and SmpB cannot target actively translating ribosomes because the downstream mRNA would directly compete for binding with SmpB. In agreement with the structure, kinetic experiments showed that the longer the downstream mRNA, the lower the rate of peptidyl transfer to tmRNA: peptidyl transfer rate on mRNA with 12 nucleotides downstream of the P-site codon was 10-fold slower than ones with 3 to 6 nucleotides downstream[19]. This specificity prevents trans-translation from interfering with productive protein synthesis.

Interestingly, the stability of a nonstop mRNA in *E. coli* is much lower compared to a normal mRNA in WT strains. In *E. coli*, rescue of ribosomes stalled on nonstop transcripts is linked to degradation of the nonstop message itself. The trans-translation pathway is thought to recruit a nuclease to target the problematic mRNA for degradation in *E. coli*[20] (Fig 1.1). Work by Karzai has argued that RNase R gets recruited to nonstop messages by tmRNA and preferentially degrades them[20,21]. This model was supported by immunoprecipitation assays with tmRNA which showed that RNase R associates with tmRNA. Reporter data also showed that nonstop reporter mRNA is stabilized in a RNase R deletion *E. coli* strain as compared to WT[22]. Overall, the trans-translation pathway selectively rescues stalled ribosomes, prevents proteotoxicity, and

degrades the truncated messages to prevent more ribosomes from translating a problematic mRNA.

1.1.2 The ArfA pathway

Sometimes the level of ribosome stalling in the cell exceeds what tmRNA can relieve, so many bacteria have a back-up pathway to compensate. This pathway involves a factor called alternative rescue factor A (ArfA). ArfA binds to ribosomes that are stalled on the 3' end of messages and recruits release factor 2 (RF2) to hydrolyze the peptide from the P-site tRNA[23–25]. Cryo-EM structures of ArfA showed that similar to SmpB, the C-terminus of ArfA extends into the mRNA channel of the small subunit indicating a similar selectivity for ribosomes stalled on the 3' end of mRNAs[26–30]. Also similar to SmpB, the activity of ArfA rescue has been shown to decrease with longer downstream mRNA[31,32]. However, in contrast to the trans-translation pathway, ArfA does not target the nascent chain nor the mRNA for degradation[23] (Fig 1.1). This means that rescue of ribosomes by ArfA results in accumulation of incomplete polypeptides. This may be why the tmRNA pathway is the dominant pathway.

ArfA itself is regulated by tmRNA to ensure that it is only expressed when tmRNA is overwhelmed or absent. The ArfA mRNA contains a RNase III cleavage site; this cleavage generates a nonstop mRNA[33]. Therefore, the ArfA transcript is normally targeted by the tmRNA pathway in *E. coli*, and thus is not expressed when tmRNA can target both the nascent peptide and the mRNA for degradation. However, when tmRNA

is overwhelmed, it cannot sufficiently suppress ArfA expression, and ArfA accumulates to high levels and relieves ribosome stalling[34].

Many bacteria contain a back-up rescue pathway similar to ArfA but identifying these back-up systems has been challenging due to the lack of sequence homology in these short proteins. In bacteria that lack a back-up system, tmRNA is an essential gene, another piece of evidence that relieving stalled ribosomes is essential for cell viability[35].

1.2 Rescue of ribosomes stalled in the middle of ORFs

Ribosomes can also encounter problems in the middle of ORFs due to inhibition of elongation by mechanisms such as antibiotic binding. These stalled ribosomes differ from ribosomes trapped on nonstop messages in that there is mRNA downstream of the ribosome. This means that the tmRNA/SmpB cannot bind because SmpB cannot insert its C-terminal tail into the mRNA tunnel. Thus, a different rescue pathway is necessary for ribosomes stalled in the middle of ORFs. Early work has showed that tmRNA also acts on ribosomes stalled internally in an ORF which was perplexing at first because tmRNA should be selective for nonstop messages. Later work by Hayes showed that the mRNA is cleaved in the A-site of the stalled ribosome in *E. coli*[36]. Although the endonuclease was not identified, mass spectrometry data showed that after cleavage, the nascent peptide was tagged with the tmRNA degron sequence[36–38]. The evidence of endonucleolytic cleavage at the stall site brought about a model where stalling would eventually lead to cleavage in a non-selective way[39]. However, mathematical modeling showed that without selectivity, protein synthesis rates would decrease even for

transcripts without an irreversible stall site[40]. Thus, a more selective model for targeting ribosomes stalled in the middle of ORFs is required to explain the protein synthesis rates observed *in vivo*. That mechanism was discovered and explained first in eukaryotes.

1.2.1 Ribosome collisions in eukaryotes

Recent work in yeast has elucidated the mechanism of how stalled ribosomes are recognized and resolved in eukaryotes. One of the major insights is that when a ribosome stalls in the middle of an ORF for long enough, an upstream ribosome collides into the stalled one. Ribosome collisions lead to stable dimers and create a unique structural interface through interactions between the two small subunits of the two ribosomes. This unique structural interface serves as a stable binding site for downstream factors to bind and signal to the cell that there is a problem with translating the mRNA. That signal is ubiquitination of several ribosomal proteins by an E3 ligase called Hel2 in yeast[41,42] (Fig 1.2).

Once the ribosomes are ubiquitinated, a complex called the ribosome quality control trigger complex (RQT) can bind by recognizing the ubiquitin. The key functional member of RQT is a 3' to 5' RNA helicase called Ski2-like helicase 1 (Slh1). Slh1 splits the collided ribosomes in yeast by exerting a pulling force on the mRNA on the stalled ribosome which forces the collided ribosome to act like a wedge to split the stalled one[43,44]. This splitting mechanism also confers selectivity because if a ribosome is not collided into the stalled ribosome, the pulling force alone cannot split the stalled ribosome[43]. This mechanism of action by Slh1 is quite unique in that its ability to split

ribosomes does not depend on the occupancy of the A-site, in contrast to rescue pathways for ribosomes stalled on nonstop messages (e.g. tmRNA/SmpB in bacteria and Dom34/Hbs1 in yeast, see below). The mechanism of action may also have evolved because many ribosomes stall internally in an ORF with an occupied A-site[43].

After splitting, the post-split large subunit still contains a folded nascent chain attached to a peptidyl-tRNA, and thus cannot simply diffuse away from the ribosome. A factor called Rqc2 binds to the large subunit by making contacts with the peptidyl tRNA as well at the interface where the small subunit would bind. This mode of binding prevents Rqc2 from acting on fully formed 80S ribosomes. Rqc2 recruits tRNAs aminoacylated with Ala or Thr and adds those residues to the nascent chain in a process called CAT-tailing[45,46]. Eventually a lysine residue is exposed out of the exit tunnel of the large subunit and another factor called Ltn1 ubiquitinates the nascent chain on the ribosome[47] (Fig 1.2). The ubiquitinated nascent chain is then released by Vms1 which cleaves the tRNA from the nascent chain[48]. This entire process results in degradation of the nascent chain by the proteasome[49].

A couple of years ago, work done in our lab showed that there is a secondary pathway in yeast that comes into play when Slh1 is overwhelmed. We discovered a factor in yeast called Cue2, an endonuclease that cleaves the mRNA between collided ribosomes[50]. Cue2 contains a CUE domain which binds to ubiquitin; therefore, Cue2 is able to bind to collided ribosomes after Hel2 ubiquitination. Cue2 also contains an SMR endonuclease domain which is responsible for cleaving the mRNA in between the collided ribosomes[50]. After cleavage, the collided ribosome becomes a substrate for

nonstop decay in eukaryotes where the ribosomes are rescued by factors, Dom34 and Hbs1[51]. Like tmRNA/SmpB, Dom34/Hbs1 is also selective for ribosomes stalled on truncated transcripts[51]. The cleavage by Cue2 also destabilizes the message, and it is rapidly degraded by exonucleases[50] (Fig 1.2). Although the Slh1 pathway has been shown to be the dominant pathway in yeast, the distinct mechanisms also argue that both pathways are needed, perhaps for different substrates. One possibility is that Cue2 may mediate rapid decay of problematic mRNAs whereas Slh1 can split ribosomes that are inhibited by antibiotics and unable to undergo peptidyl transfer.

1.2.2 Ribosome collisions in E. coli

Recently, our lab and others have shown that ribosome collisions also occur in bacteria. Our lab discovered the endonuclease involved in recognizing and rescuing ribosomes stalled in the middle of ORFs using a genetic screen. We expressed a reporter consisting of a fusion of nano-luciferase and bleomycin resistance protein. In between the two ORFs, a stalling sequence, SecM, was inserted. When ribosomes encounter the SecM sequence, they stall because the nascent chain interacts with the ribosome exit tunnel and prevents elongation[3]. The stalled ribosomes get rescued and never express the bleomycin resistance gene. This stalling reporter was transformed into an *E. coli* knockout library, and using Tn-seq approach, a factor was identified whose deletion resulted in expression of the bleomycin resistance protein. This factor is called SmrB, and interestingly like Cue2 in yeast, it contains an SMR endonuclease domain[52].

Our work showed that SmrB binds preferentially to collided ribosomes. When cells are treated with low doses of elongation inhibitors only some ribosomes are stalled and thus collisions can occur; in contrast, with high doses of elongation inhibitors, all ribosomes are stalled[41]. When SmrB binding to ribosomes was observed over sucrose gradients with lysates from cells treated with various doses of elongation inhibitors, SmrB was bound deep in the gradient only at the low dose regime[52]. We also showed that SmrB cleaves in between the collided ribosomes by 5' and 3' rapid amplification of cDNA ends (RACE). This cleavage generates a non-stop message that is rescued by tmRNA through the mechanism described previously[52]. This process ensures that the ribosomes are recycled, and the nascent peptide is tagged for degradation by ClpXP. The cleavage by SmrB also destabilizes the problematic mRNA similar to Cue2 cleavage in yeast [50]. This whole process in *E. coli* results in rescue of the collided ribosomes and degradation of the nascent peptide and problematic mRNA.

With the help of our collaborators, the first structure of the *E. coli* collided ribosome was solved by cryo-EM which showed remarkable resemblance to the eukaryotic collided ribosomes with the collision interface comprised of the two small subunits. The Beckmann lab also solved the disome structure with SmrB bound which gave insights into its mechanism of action and how SmrB distinguishes collided ribosomes over elongating ribosomes. SmrB uses its N-terminal tail to sample all ribosomes, but the SMR domain only stably binds to the collision interface making contacts with both the stalled and collided ribosomes. SmrB is also positioned so that the catalytic residues of the SMR domain are in position to cleave the mRNA in between

the collided ribosomes[52]. Additionally, during our work on SmrB, our collaborators also solved the structure of the *B. subtilis* collided disome which indicated that ribosome collisions are conserved in bacteria[52]. However, whether the rescue machinery that recognizes collided ribosomes is conserved was unknown.

1.3 Ribosome rescue in *B. subtilis*

1.3.1 Trans-translation and backup pathways in B. subtilis

The trans-translation pathway is conserved in nearly all bacteria. *B. subtilis* tmRNA works with SmpB to bind to ribosomes stalled on nonstop messages and rescue them. The ORF of the *B. subtilis* tmRNA also encodes for a degron tag, albeit a different sequence (AGKTNSFNQNVALAA) than the one in *E. coli*; this tag ensures that the nascent chain is degraded by ClpXP. It also contains a canonical stop codon for the ribosome and nascent chain to be released[53–55]. Although the importance of tmRNA under conditions of stress and sporulation has been studied in *B. subtilis*, the stability of nonstop messages as compared to normal mRNAs has not been studied. Whether nonstop messages are preferentially decayed and whether RNase R is also involved is not known.

The backup rescue pathway in *B. subtilis* was discovered recently[56]. Bacillus ribosome-rescue factor A (BrfA) does not share sequence similarity to ArfA but shares a similar function. BrfA also rescues ribosomes stalled on nonstop messages by recruiting RF2 to hydrolyze the peptidyl-tRNA and release the nascent chain without targeting it for degradation. Remarkably, BrfA's expression itself is regulated by tmRNA; only when

tmRNA is overwhelmed does BrfA expression become stabilized. One difference is that the BrfA transcript does not contain a RNase cleavage site; instead, it is regulated by tmRNA because of an internal transcription termination event which creates the nonstop message[56]. The conservation of a backup rescue pathway in *E. coli* and *B. subtilis* highlights the importance of rescuing ribosomes stalled on nonstop messages.

1.3.2 Ribosome collisions in B. subtilis

In recent years, a homolog of Rqc2 was identified to be present in *B. subtilis* called RqcH[57]. Rqc2 homologs are found in various phyla of bacteria and archaea and may be a part of ribosome quality control in all domains of life[57,58]. Resembling Rqc2's mechanism of action, RqcH binds to a large subunit that contains a nascent chain and peptidyl-tRNA still attached. RqcH recruits Ala-tRNAs to add alanines to the nascent chain in a process called Ala-tailing[57]. This addition of alanines is thought to continue until the nascent chain is hydrolyzed from the tRNA, and the Ala-tailed nascent chain is released[59–61]. This hydrolase has recently been proposed to be Pth in bacteria[62]. Alanine tails serve as a degradation tag for the peptide to be degraded by the ClpXP protease[59–61]. The similarities of alanine-tailing and CAT-tailing showed that the RQC pathway in *B. subtilis* may be quite similar to that of eukaryotes. However, it was unknown what the splitter like yeast Slh1 was in *B. subtilis*.

Recently, work from another lab showed that there is also an SMR domain protein in *B. subtilis* that may be involved in rescuing these collided ribosomes[63]. This protein called MutS2 contains an SMR domain like SmrB in *E. coli*, but the rest of the

protein's domain architecture is quite different. MutS2 is a paralog of the DNA mismatch repair protein MutS, but MutS2 has been shown to not be involved in mismatch repair because it lacks the mismatch recognition domains that MutS contains[64]. MutS2 has a Core/Clamp, ABC ATPase domain, KOW, and SMR domain. The partial structure solved by the Pfeffer group showed that the Core/Clamp and ABC ATPase domains of MutS2 bind as a dimer mainly to the large subunit of the stalled ribosome[63]. Although this partial structure gave some insights on how the ATPase domain may be involved in RQC in *B. subtilis*, the exact mechanism of action of MutS2 was still unknown, as well as how MutS2 recognizes collided ribosomes versus normal elongating ribosomes. The roles of the KOW and SMR domains were also unknown. Where is the SMR domain binding, and is it cleaving the mRNA like it does in *E. coli*?

1.4 Motivating Questions

The current existing landscape of information raises several questions about ribosome rescue in *B. subtilis*. The first is: what is the mechanism of action of MutS2 in rescuing collided ribosomes? Does it split the ribosomes into subunits using its ATPase domain, or does it cleave the mRNA in between via its SMR domain or both? Recent work from our lab has made progress on elucidating the mechanism of SmrB in *E. coli*, but it is unknown if *B. subtilis* MutS2 utilizes a similar mechanism or a distinct one. Along those lines, the second question is about the fate of the mRNA in the trans-translation rescue pathway in *B. subtilis*. Do non-stop messages get preferentially degraded in *B. subtilis* as they do in *E. coli*? Previous work on trans-translation in *B. subtilis* have

focused on the fate of the nascent peptide which get tagged at degraded by ClpXP similar to that in *E. coli*.

The work presented here in *Chapter 2: B. subtilis MutS2 Splits Stalled Ribosomes into Subunits without mRNA Cleavage* is motivated by the first question. This chapter elucidates the mechanism of action of MutS2 on stalled ribosomes using *in vivo* stalling reporter and biochemistry. In collaboration with the Beckman lab, the structure of the SMR and KOW domains further characterize their role in rescuing stalled ribosomes.

To elucidate the differences of the trans-translation rescue pathways in *E. coli* and *B. subtilis*, the same non-stop reporter was introduced to both bacteria. Using western and northern blotting, the fates of the reporter protein and mRNA in each strain can be directly compared. Also, *E. coli* and *B. subtilis* contain different exo- and endonucleases for mRNA decay. Deletions of several of these nucleases reveal differences to what previous works have shown with nonstop mRNA associated nucleases.

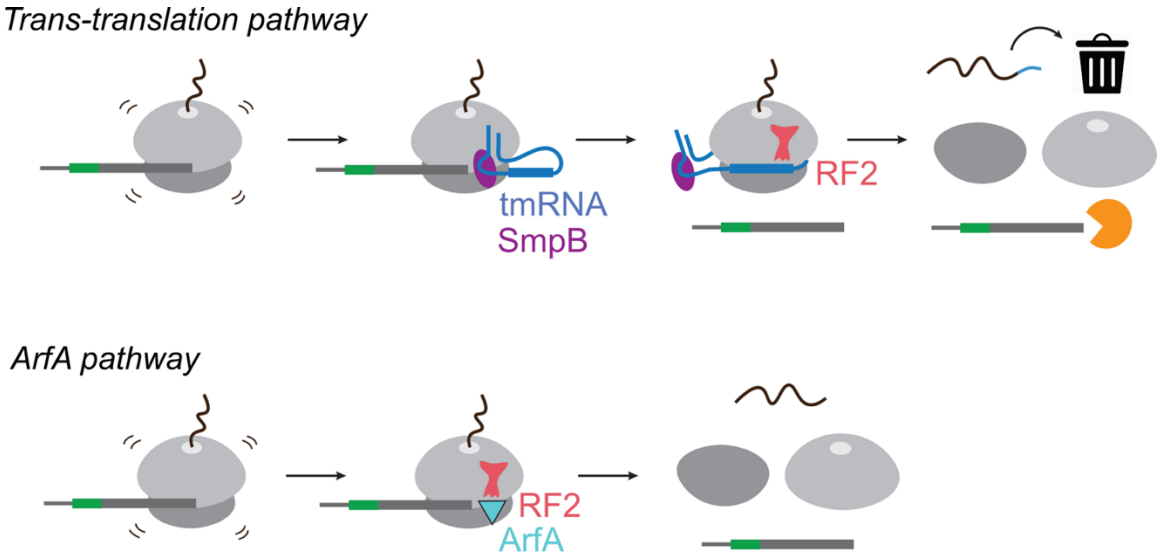
Trans-translation pathway
tmRNA
SmpB
RF2
ArfA pathway
RF2
ArfA

Figure 1.1 The trans-translation and ArfA pathways of rescuing ribosomes stalled on nonstop mRNAs.

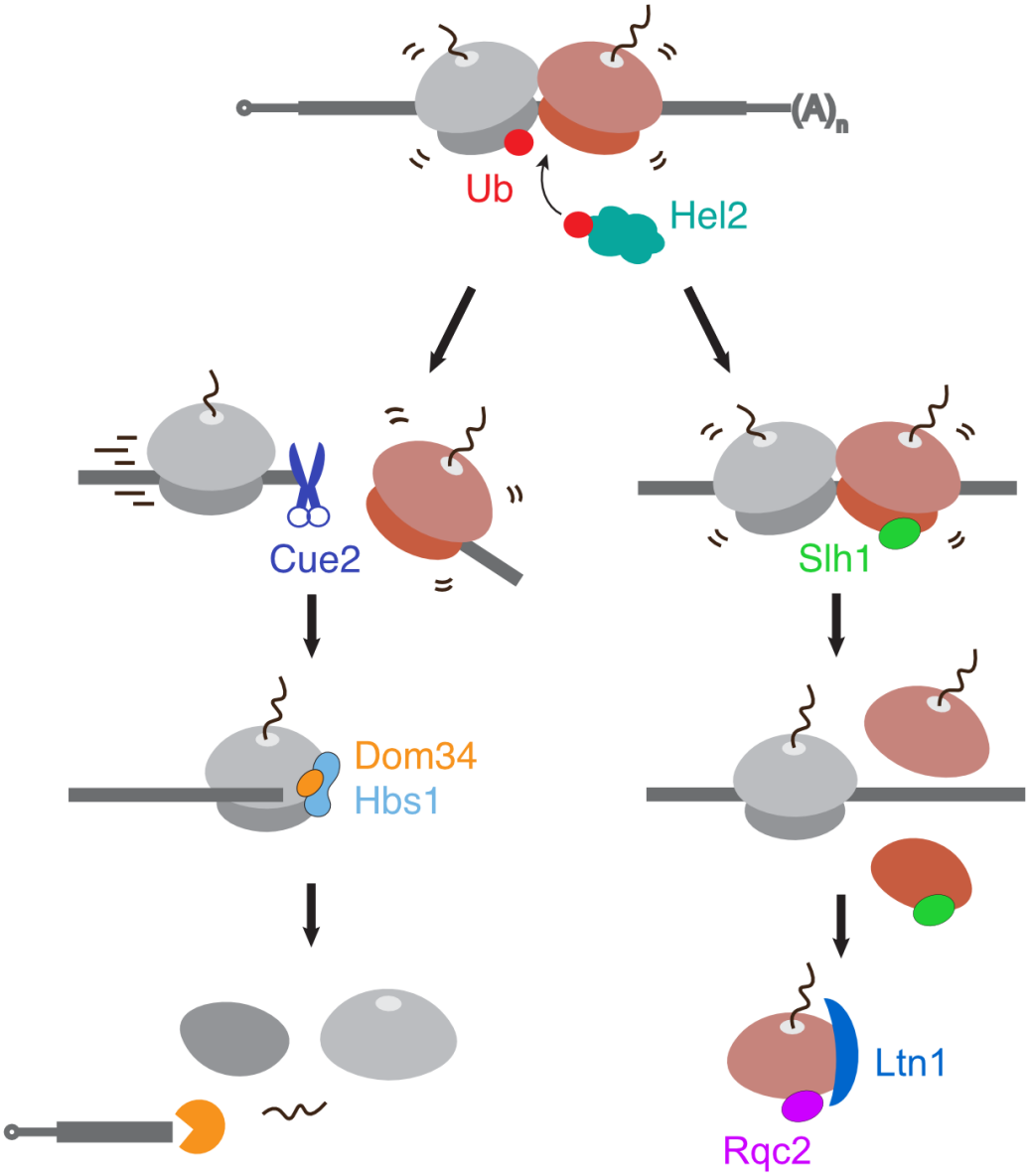
(A)n
Ub
Hel2
Cue2
Slh1
Dom34
Hbs1
Ltn1
Rqc2

Figure 1.2 Rescue pathways of collided ribosomes in *S. cerevisiae*

Chapter 2: *B. subtilis* MutS2 Splits Stalled Ribosomes into Subunits without mRNA Cleavage

Note: Text and data in this chapter was used to publish in the EMBO Journal

2.1 Introduction

In bacteria, translating ribosomes stall when they encounter problems with an mRNA template, such as nucleotides that are chemically damaged and therefore unreadable, or truncations of the mRNA that result in the loss of the stop codon[9,10]. Ribosomes also stall when elongation is slowed by low concentrations of aminoacyl-tRNA at clusters of rare codons or by specific peptide sequences that are difficult for the active site to accommodate (such as polyproline sequences)[3,65–67]. Indeed, certain arrest peptides such as SecM and TnaC take advantage of reversible ribosome stalling as a means to regulate the expression of downstream genes[68–71]. In addition, bacterial ribosomes are arrested by many antibiotics[72,73]. If left unresolved, ribosome stalling by any of these mechanisms can be dangerous to the cell because it reduces the pool of active ribosomes and leads to the production of truncated, potentially toxic proteins.

Over the course of evolution, these problems imposed selective pressure that favored the emergence of dedicated pathways that rescue stalled ribosomes. These pathways accomplish the twin tasks of recovering the ribosomes and targeting the

truncated nascent peptides and problematic mRNAs for degradation[74]. The best-characterized pathway in bacteria involves transfer messenger RNA (tmRNA) which selectively rescues ribosomes stalled at the end of truncated mRNAs lacking a stop codon (so-called "nonstop" messages)[17,19]. The ribosome resumes translation using tmRNA as a template, adding a peptide tag to the nascent polypeptide that targets it for degradation by proteases, primarily ClpXP[14]. Nearly all bacterial genomes encode tmRNA. There are also backup mechanisms that become engaged when tmRNA is overwhelmed. In *E. coli* and in *B. subtilis*, the backup pathway involves a small protein (ArfA/BrfA, respectively) that recruits a release factor to hydrolyze the nascent peptidyl-tRNA and promote recycling of the ribosome subunits without targeting the peptide for degradation[23,33,56]. Both of these pathways show a preference for ribosomes stalled on truncated mRNAs and require that the active site of the ribosome be competent to catalyze peptidyl transfer (for tmRNA) or peptidyl hydrolysis (for ArfA). In *E. coli*, previous work has shown that tmRNA recruits an exonuclease, RNase R, to degrade the nonstop message[20–22]. Thus, in *E. coli*, nonstop mRNAs are drastically less stable than full-length mRNAs. However, the stability of nonstop mRNA has not been investigated in *B. subtilis*.

Several bacteria, including *B. subtilis*, also have a distinct pathway that shares similarities to the eukaryotic pathway known as ribosome-associated quality control (RQC). In eukaryotes, stalled ribosomes are split into subunits, yielding a free small subunit and a large subunit with a trapped peptidyl-tRNA[44,75]. A factor called Rqc2 in yeast then catalyzes the addition of C-terminal Ala and Thr tails (CAT tails) to the

nascent peptide, translocating the peptide out of the tunnel such that encoded Lys residues can be tagged with ubiquitin by Ltn1 and ultimately degraded by the proteasome[45,46,76]. In a similar fashion, *B. subtilis* contains a homolog of Rqc2 called RqcH which binds to dissociated 50 S subunits with peptidyl-tRNA trapped on them and catalyzes the addition of Ala residues (Ala-tails) to the nascent peptide[57,59–61]. Like the tmRNA tag, these Ala-tails target the nascent peptide for degradation by the bacterial proteasome equivalent, ClpXP. Many questions remain regarding how the RQC pathway operates in bacteria including: (1) what are the natural substrates of this pathway and how are they recognized, (2) how are stalled ribosomes split in order to generate the 50S-peptidyl-tRNA substrate for RqcH, and (3) how is the nascent peptide hydrolyzed from the tRNA and released.

We recently showed that ribosome rescue in *E. coli* is triggered by collisions that occur when a trailing ribosome catches up to a stalled ribosome[52]. The stable interaction between the two ribosomes (primarily through their 30 S subunits) creates a new interface that recruits a factor called SmrB. This factor has an SMR domain that performs endonucleolytic cleavage of mRNAs when bound between collided ribosomes; cleavage occurs just upstream of the stalled ribosome. This cleavage in the ORF creates a nonstop mRNA such that upstream ribosomes that translate to this newly formed 3'-end are rapidly rescued by tmRNA. In addition to the cryo-EM structure of *E. coli* collided ribosomes bound to SmrB, we also reported the structure of collided ribosomes from *B. subtilis*, arguing that collisions are a conserved mechanism for recognizing stalled ribosomes in bacteria[40], much like in yeast and human cells[41,42,52,77].

Pfeffer and Joazeiro also reported the structure of collided ribosomes from *B. subtilis* bound to a factor homologous to SmrB called MutS2[63]. Like SmrB, MutS2 contains an SMR domain, but unlike SmrB it also contains several other domains including an ABC ATPase domain. The structure revealed that MutS2 binds to collided ribosomes as a dimer and that its ATPase domains contact the lead ribosome[63]. These observations raised the exciting possibility that MutS2 recognizes collided ribosomes specifically and uses its ATPase domain to split the stalled ribosomes into subunits. Thus, MutS2 could be the missing factor required to dissociate ribosomes to promote Ala-tailing by RqcH. It remained unclear, however, how MutS2 selectively binds collided ribosomes since the ATPase domains bind to the lead ribosome alone and the SMR domain was not resolved in their structure. Furthermore, these studies did not establish whether MutS2 cleaves mRNA using its SMR domain as we had observed with E. coli SmrB[63].

Here, we thoroughly characterize the role of MutS2 in ribosome rescue in *B. subtilis*. We show that MutS2 is recruited by ribosome collisions and report the cryo-EM structure of the SMR and KOW domains of MutS2 bound to collided ribosomes. We find that the SMR domain plays an important role in recruiting MutS2 to collided ribosomes. Using a reporter construct *in vivo*, we show that MutS2 uses its ATPase activity to split ribosomes into subunits, promoting Ala-tailing of the nascent peptide by RqcH. Importantly, we see no evidence of mRNA cleavage by MutS2, arguing that it does not act upstream of the tmRNA pathway as SmrB does in *E. coli*. Finally, we reconstitute the "rescue" reaction *in vitro* using purified collided ribosomes and show that MutS2 splits

the stalled ribosomes into subunits in an ATP-dependent fashion but lacks detectable endonuclease activity. These findings define the biochemical activities of MutS2 in ribosome rescue in *B. subtilis*.

2.2 Materials and Methods

2.2.1 Bacterial strains and plasmids

Knockout strains for *B. subtilis* were obtained from the Bacillus Genetic Stock Center (BGSC)[78]. Knockout strains for *E. coli* MG1655 were constructed using one-step genomic replacement with a PCR fragment with Lambda Red recombinase (PMID: 10829079) and verified by PCR. The reporter constructs and CamR marker were introduced into the amyE locus through recombination for B. subtilis[79] and verified by PCR and Sanger sequencing. All *B. subtilis* reporter constructs were expressed from a P_{veg} promoter and a strong ribosome binding site (RBS)[80]. For *E. coli*, the reporter constructs were expressed from plasmids containing AmpR marker and p15A origin of replication. N-terminal Flag-tagged versions of MutS2 with a spectinomycin resistance marker were introduced into *ΔmutS2* cells into the thrC locus with the endogenous mutS2 5' UTR and terminator by recombination[79] and confirmed by PCR and Sanger sequencing.

2.2.2 Spotting assays

Cells were grown overnight at 37 °C in liquid LB. The overnight cultures were diluted to prepare five-fold serial dilutions starting from OD600 = 0.005. Subsequently, 1.5 µL of the diluted cultures was spotted on LB plates with or without various antibiotics. Plates were then incubated at 37 °C overnight.

2.2.3 Polysome profiling

B. subtilis cells were cultured at 37 °C in 500 mL of LB to OD_{600} = 0.45, at which point the cells were treated for 5 min with antibiotics at the concentrations indicated in the figures. Cells were harvested by filtration using a Kontes 99-mm filtration apparatus with a 0.45-µm nitrocellulose filter (Whatman) and flash-frozen in liquid nitrogen. Cells were then lysed in lysis buffer (20 mM Tris pH 8.0, 10 mM $MgCl_2$, 100 mM NH_4Cl, 5 mM CaCl2, 0.4% Triton X-100, 0.1% NP-40, 1 mM CAM, 100 U ml^{-1} DNase I) using a Spex 6875D freezer mill with six cycles of 1 min grinding at 6 Hz and 1 min cooling. Lysates were centrifuged at 20,000 G for 10 min at 4 °C to pellet cell debris. Samples that were subjected to RNase A digestion to detect nuclease-resistant disomes were incubated for 1 h at 25 °C with 15 µL of RNase A (1:1000 dilution) then treated with 6 µL of SUPERaseIn RNase Inhibitor (Thermo Fisher). Sucrose gradients of 10–50% were prepared using a Gradient Master 108 (Biocomp) with gradient buffer (20 mM Tris pH 8.0, 10 mM $MgCl_2$, 100 mM NH_4Cl, 2 mM DTT). Then, 15–30 AU of lysate was loaded on top of the sucrose gradient and centrifuged in an SW 41 rotor at 35,000 rpm for 2.5 h at 4 °C. Fractionation was performed on a Piston Gradients Fractionator (Biocomp). To process each fraction for western blots, proteins were precipitated in 10% TCA. After

pelleting, pellets were washed twice in ice-cold acetone and vacuum-dried for 5 min. Finally, we resuspended each pellet in 6X loading dye and neutralized the solution with Tris-HCl pH 7.5. Samples were probed on western blots using an anti-Flag-HRP antibody (1:2000 dilution) and detected using SuperSignal West Femto Maximum Sensitivity Substrate (Thermo Fisher) and visualized using the ChemiDoc Imaging System (Biorad).

2.2.4 Western blots

E. coli and *B. subtilis* cells were grown in LB with appropriate antibiotics to OD600 ~ 0.5-1. In total, 1mL of culture was harvested by centrifugation, resuspended in appropriate lysis buffer (*E. coli* lysis buffer: 12.5 mM Tris pH 6.8 with 4% SDS; *B. subtilis* lysis buffer: 100 mM NaCl, 50 mM EDTA). For *E. coli*, the samples were lysed by heating to 90 C for 10 min. For *B. subtilis*, the samples were lysed with 7 μL of 10 mg/mL lysozyme and incubates at 37 C for 30 min, and then, 40 μL of 20% sarkosyl was added and incubated for an additional 5 min. 6X loading dye (250 mM Tris pH 6.8, 20% glycerol, 30% β-mercaptoethanol, 10% SDS, saturated bromophenol blue) was added to all samples and denatured at 90 C for 10 min. Proteins were separated on a 4–12% Criterion XT Bis-Tris protein gel (Bio-Rad) with XT-MES buffer and transferred to polyvinylidene membranes using the Trans-Blot Turbo Transfer system (Bio-Rad). Membranes were blocked in 5% milk for 1 h at room temperature, washed, and then probed with antibodies diluted in TBS-Tween at the following dilutions: anti-NanoLuc, 1:2,000 (Promega); anti-FtsZ, 1:2000 (Sigma); anti-RpoB, 1:1000 (BioLegend); anti-mouse-HRP, 1:4000 (Thermo Fisher); anti-rabbit-HRP, 1:4000 (Santa Cruz

Biotechnologies). Chemiluminescent signals from HRP were detected using SuperSignal West Pico PLUS Chemiluminescent Substrate (Thermo Fisher) or SuperSignal West Femto Maximum Sensitivity Substrate (Thermo Fisher) and were visualized using the ChemiDoc Imaging System (Bio-Rad).

2.2.5 Northern blots

Cells were grown in LB to OD_{600} = 0.5, an equal volume of ice-cold methanol was added for *B. subtilis* harvesting, and the samples were harvested by centrifugation. Pellets were frozen on dry ice and stored at −80 °C. Pellets were then thawed on ice and resuspended in appropriate lysis buffer (*E. coli* RNA lysis buffer: 10 mM Tris pH 8, 0.1 mM EDTA, 100 mM NaCl, 1% SDS; *B. subtilis* RNA lysis buffer: 30 mM Tris pH 8.0, 10 mM EDTA). An equal amount of lysis buffer with 10 mg ml^{-1} lysozyme was added to the B. subtilis lysates and incubated at 37 °C shaking at 1000 rpm for 30 min. RNA was extracted twice with phenol (pH 4.5) first at 65°C and then at room temperature, followed by chloroform extraction. The RNA in the aqueous layer was precipitated with isopropanol and 0.3 M sodium acetate (pH 5.5), washed with 80% ethanol, and resuspended in water. The purified RNA was separated on a 1.2% agarose-formaldehyde denaturing gel and was then transferred to a nylon membrane (Hybond-N + , Cytvia) in 10X SSC buffer using a model 785 vacuum blotter (Bio-Rad). RNA was cross-linked to the membrane using an ultraviolet (UV) crosslinker (Stratgen). Pre-hybridization and hybridization were performed in PerfectHyb Plus Hybridization Buffer (Sigma). The RNA was probed with 50–150 nM 5’-digoxigenin-labeled DNA oligonucleotides (IDT).

Digoxigenin was detected with anti-digoxigenin-AP antibodies diluted 1:500–1:1000 (Sigma). Chemiluminescent signals from alkaline phosphatase were detected with CDP-star (Sigma) and were visualized using the ChemiDoc Imaging System (Bio-Rad).

2.2.6 MS analysis of tagging sites on the reporter protein

Strains expressing the ApdA reporter were grown in 100 mL of LB with 20 µM bortezomib until OD_{600} = 0.5 and harvested by centrifugation. The pellet was frozen at −80 °C and thawed in 2X CellLytic B-cell lysis reagent (Sigma) and 0.2 mg mL^{-1} lysozyme for 10 min. The lysate was clarified by centrifugation for 30 min at 20,000 G at 4 °C. In total, 50 µL of Streptactin Sepharose beads (IBA) were added to the supernatant and samples were incubated at 4 C for 1 h. The beads were washed four times with IP wash buffer (20 mM Tris pH 8.0, 100 mM NH_4Cl, 0.4% Triton X-100, 0.1% NP-40) for 5 min at 4 °C. Protein was eluted from the beads by shaking at 4 °C in elution buffer (20 mM Tris pH 8.0, 100 mM NH_4Cl, 5 mM desthiobiotin) for 1 h. Then, 36 µL of the immunoprecipitated sample was reduced with 100 mM DTT in 100 mM triethylammonium bicarbonate (TEAB) buffer at 58 °C for 55 min and then the pH was adjusted to 8.0. The samples were alkylated with 200 mM iodoacetamide in 100 mM TEAB buffer in the dark at room temperature for 15 min. Proteins were pelleted and resuspended in 50 mM TEAB and proteolyzed with 15 ng μL^{-1} of LysC (Wyco) at 37 °C overnight. Peptides were desalted on Oasis u-HLB plates (Waters), eluted with 60% acetonitrile (ACN)/0.1% trifluoracetic acid (TFA), dried and reconstituted with 2% ACN/0.1% formic acid.

2.2.6.1 LC-MS/MS analysis

Desalted peptides cleaved by LysC were analyzed by LC-MS/MS. Then peptides were separated by reverse-phase chromatography (2–90% ACN/0.1% formic acid gradient over 63 min at a rate of 300 nL min^{-1}) on a 75 µm × 150 mm ReproSIL-Pur-120-C18-AQ column (Dr. Albin Maisch, Germany) using the nano-EasyLC 1200 system (Thermo). Eluting peptides were sprayed into an Orbitrap-Lumos_ETD mass spectrometer through a 1-µm emitter tip (New Objective) at 2.4 kV. Scans were acquired within 350–1600 Da m/z targeting the truncated reporter with 15 s dynamic exclusion. Precursor ions were individually isolated and were fragmented (MS/MS) using an HCD activation collision energy of 30. Precursor (fragment) ions were analyzed at a resolution of 200 Da of 120,000 with the following parameters: max injection time (IT), 100 ms (resolution of 30,000) in three cycles. The MS/MS spectra were processed with Proteome Discover v2.4 (Thermo Fisher) and were analyzed with Mascot v.2.8.0 (Matrix Science) using RefSeq2021_204_Bacillus.S and a database with peptides from the NanoLucBleR reporter protein. Peptide identifications from Mascot searches were processed within the Proteome Discoverer-Percolator to identify peptides with a confidence threshold of a 5% false discovery rate, as determined by an auto-concatenated decoy database search.

2.2.7 Purification of MutS2

N-terminally His-tagged versions of MutS2 were expressed from pET24d(+) plasmids in BL21(DE3) *E. coli* cells. Cells were grown in 9 L LB medium to approximately OD_{600} = 2.5 and MutS2 expression was induced with IPTG (1 mM). Cells were harvested by centrifugation and resuspended in 30 mL lysis buffer (20 mM HEPES pH 7.5, 95 mM KCl, 5 mM NH_4Cl, 10 mM $Mg(OAc)_2$, 1mM DTT, protease inhibitor (Roche)), then lysed using a microfluidizer (15k psi, H10Z, Microfluidics). Lysates were cleared by centrifugation (16,000 rpm, 20 min, 4 °C, Sorvall SS-34 rotor). Cleared lysates were applied to 3 mL TALON Metal Affinity Resin (Takara) and incubated for 30 min at 4 °C. The resin was washed with 40 mL each of wash buffer (50 mM HEPES pH 7.5, 225 mM NH_4Cl, 20 mM $MgCl_2$, 0.1 mM PMSF, 5% glycerol, 1 mM DTT, 20 mM imidazole, 0.4% Triton X-100, protease inhibitor), wash buffer with 1 M KCl, and wash buffer without imidazole or Triton X-100, sequentially. The protein was eluted by incubation with 5 mL wash buffer with 150 mM imidazole, followed by a second elution with 200 mM imidazole. Elution fractions were analyzed by Superdex 200 gel filtration and fractions containing pure MutS2 protein were pooled, concentrated using an Amicon 50 kDa MWCO concentrator, and used for the cryo-EM and subunit splitting experiments.

2.2.8 B. subtilis translation extract preparation

Bacillus subtilis strain 168 *Δhpf ΔssrA ΔSAS1-2* cells were grown on an LB agar plate containing 5 µg/mL CAM, 1 µg/mL erythromycin and 10 µg/mL kanamycin at 37 °C. Six 2 L flasks with LB medium supplemented with 1% glucose were inoculated to an OD_{600} of 0.02 and incubated at 37 °C. Cells were harvested during the exponential

growth phase at an OD_{600} between 1 and 2 by centrifugation at 8000 rpm for 5 min at room temperature. Cells were resuspended in 1X PBS, combined into one bottle, and pelleted again. Cells were resuspended in lysis buffer (10 mM HEPES-KOH pH 8.2, 60 mM K-glutamate, 14 mM $Mg(OAc)_2$ and 20 µg/mL DNase I). Cells were lysed by one pass through a cell disruptor (Constant Systems) at 18,000 psi at room temperature, with the lysate collected on ice. Lysate was centrifuged in an SS-34 rotor at 18,000 rpm for 15 min at 4 °C. Extracts were frozen in liquid nitrogen and stored at −80 °C.

2.2.9 Preparation of mRNA construct

mRNA was prepared by PCR amplification of DNA template followed by *in vitro* transcription and precipitation of mRNA using LiCl. For *B. subtilis* disomes, an mRNA was transcribed from pMAT MifM_WT_V5 encoding a His-tag, 3C cleavage site, V5 tag for detection, and MifM stalling sequence. The forward primer was MifM_for2, annealing to the T7 promoter. For short/standard length mRNA used in splitting assays, a reverse primer was used to append four stop codons immediately downstream of the stalling sequence (MifM_rev2). *In vitro* transcription reactions were set up in 100 µL reactions with 2 µg DNA, 3 µg T7 RNA Polymerase and performed in 40 mM Tris pH 7.9, 2.5 mM Spermidine, 26 mM $MgCl_2$, 0.01% Trition X-100, 5 mM DTT, 8 mM each ATP, GTP, CTP, UTP, and 0.4 U/µL SUPERaseIn RNase Inhibitor (Invitrogen). Reactions were incubated for 4 h at 37 °C. RNA was precipitated by the addition of 150 µL 7 M LiCl and incubated at −20 °C overnight, then washed with 70% ethanol and resuspended in water.

2.2.10 B. subtilis in vitro translation and isolation of disomes

Disomes were generated by performing *in vitro* translation with an mRNA featuring a MifM stalling sequence and His-tag for purification of programmed ribosomes via the nascent chain. *In vitro* translation reactions were prepared at room temperature in a final volume of 12 mL, with 4700 A_{260} units cell extract, 480 µg mRNA, 50 mM HEPES pH 8.2, 10 mM NH_4OAc, 130 mM potassium acetate, 30 mM sodium pyruvate, 4 mM sodium oxalate, 50 µg/mL tRNA (from *E. coli* MRE 600 – Sigma 10109541001), 0.2 mg/mL folinic acid, 0.1 mg/mL creatine kinase, 20 mM creatine phosphate, 4 mM ATP, 3 mM GTP, 0.15 mM amino acids, 1 mM DTT, 0.08 U/mL SUPERaseIn RNase Inhibitor (Invitrogen), 1% PEG 8000 and magnesium acetate (typically 16-20 mM in addition to that present in extract, determined by performing test translations monitored by Western blot). The reaction was split to 1 mL aliquots, and incubated at 32 °C for 40 min, shaking at 1000 rpm. *In vitro* translation reaction was incubated at 4 °C for 1 h with TALON resin (3.8 mL slurry) that had been washed with buffer A (30 mM HEPES pH 7.5, 100 mM KOAc, 10 mM Mg(OAc)2, 0.2% DDM) and, incubated with *E. coli* tRNA to reduce non-specific binding of ribosomes. Talon beads were then washed with 30 mL buffer A supplemented with 20 mM imidazole. Elution was performed by cleavage with 3C protease (3.3 mg in 5 mL buffer A) at 4 °C. The sample was loaded on 10–50% sucrose gradients prepared in buffer A and centrifuged overnight in a SW40 rotor at 4 °C (for an equivalent of 3 h at 40,000 rpm). Gradients were fractionated on a Biocomp Gradient Station and the disome peak was collected. Disomes were pelleted in a TLA110 rotor for 1 h at 100,000 rpm at 4 °C and resuspended

in 25 mM HEPES pH 7.5, 150 mM KOAc, 10 mM $Mg(OAc)_2$, 2 mM DTT. If not used immediately, disomes were frozen in liquid nitrogen and stored at −80 °C.

2.2.11 In vitro reconstitution of the MutS2-disome complex

His-MutS2 WT was added to purified disomes from *B. subtilis* in ten-fold excess in reaction buffer (50 mM HEPES/KOH pH 7.5, 75 mM KOAc, 5 mM $Mg(OAc)_2$, 1.2mM DTT, 45 mM NH_4Cl, 4 mM $MgCl_2$, 1% glycerol, 1 mM $MnCl_2$, 1 mM AMP-PNP) and the mixture was incubated at 30 °C for 1 h. Following this, the sample was directly vitrified for cryo-EM by plunge-freezing using a Vitrobot Mark IV (FEI Company/Thermo Fisher) with an incubation time of 45 s and blotting for 2.5 s at 4 °C and a humidity of 95%.

2.2.12 Purification of cross-linked FLAG-MutS2-disome complexes from Bacillus subtilis for cryo-EM

B. subtilis cells expressing N-terminally FLAG-tagged MutS2 with the E416A mutation in the Walker B motif were grown in 4 L LB medium supplemented with kanamycin for selection to an OD of 1.5. Cells were spun down at 7800 G for 10 min at room temperature. Pellets were washed with PBS and pooled, then pelleted again and frozen in liquid nitrogen. Frozen pellets were thawed and resuspended in lysis buffer (20 mM HEPES/KOH pH 7.5, 100 mM KCl, 15 mM $Mg(OAc)_2$, 1 mM DTT, 2 mM spermidine, protease inhibitor cocktail). Cell lysis was performed in a cell disruptor (Constant Systems) at 20,000 psi at room temperature. The following steps were performed at 4 °C. Lysates were cleared by centrifugation at 27,000 G for 15 min. Cleared lysates were

incubated with 250 µL Anti-FLAG M2 Affinity Gel (Sigma) equilibrated in lysis buffer for 2 h on a wheel. Beads were recovered by centrifugation at 1380 G for 3 min and washed with 10 mL lysis buffer as a batch, then transferred to a G-25 column (MoBiCol). The column was washed twice with 10 mL lysis buffer. Elution by incubating with 50 µL FLAG peptide (145 µg/mL) in lysis buffer for 1 h. Samples were recovered by centrifugation of the column at 376 G for 2 min. Crosslinking was performed by adding 0.5 mM BS3 to the sample and shaking lightly at 10 °C for 30 min. The reaction was quenched by the addition of 25 mM Tris/HCl (pH 7.5) before vitrification. Vitrification of the sample was performed as described for the reconstituted samples.

2.2.13 Cryo-EM analysis of in vitro reconstituted sample

2.2.13.1 Data collection

Data were collected on a Titan Krios G3 (Thermo Fisher) equipped with a K2 direct detector (Gatan) at 300 keV using the semiautomated data acquisition software EPU (Thermo Fisher). 40 frames with a dose of 1.09 e-/Å2 per frame were collected in a defocus range of −0.4 to −3.5 µm. Magnification settings resulted in a pixel size of 1.045 Å/pixel. Frame alignment was executed with MotionCor2[81] and the estimation of the contrast transfer function (CTF) was performed with Gctf[82].

2.2.13.2 Processing

After the manual screening of micrographs, 5784 were selected for particle picking using Gautomatch (http://www.mrclmb.cam.ac.uk/kzhang/) with a set of reference images generated from a *B. subtilis* disome model from Saito *et al*. After 2D classification in Relion 3.1[83], 96,678 particles representing collided disomes were selected for further processing. After several rounds of 3D classification and refinement in Relion in order to remove classes without a rigid disome interface or density for the mRNA in the inter-ribosomal space, a class of 11,749 particles displaying a significant extra density next to the inter-ribosomal mRNA were selected for high-resolution refinement in CryoSPARC[84]. Homogenous refinement and focused refinement yielded a final reconstruction of the collided disome bound by the MutS2 KOW and SMR domains at an overall resolution of 3.8 Å.

2.2.13.3 MutS2 model building

In order to verify the identification of the extra densities observed in the reconstruction of the *B. subtilis* disome as MutS2, structures of the SMR and KOW domains of MutS2 as predicted by Alphafold2[85] were fitted as rigid bodies into the densities in UCSF ChimeraX[86]. A model of the collided disome bound by MutS2 was generated by adding these models to the model of a collided *B. subtilis* disome[52] and refining the resulting model in Phenix 1.20.1[87] after minor adjustments using WinCoot 0.8.9.2 and ISOLDE for ChimeraX, based on the experimental data.

2.2.14 Cryo-EM analysis of cross-linked native sample

Data were collected on a Titan Krios TEM equipped with a Falcon II DED at 300 kV. Ten frames with a dose of 2.5 e-/Å2 per frame were collected in a defocus range of −0.5 to −4.0 µm. Magnification settings resulted in a pixel size of 1.09 Å/pixel. Frame alignment was executed with MotionCor2[81] and the estimation of the contrast transfer function (CTF) was performed with Gctf[82]. After manual screening of micrographs, 11,923 were selected for particle picking using Gautomatch with a set of reference images generated from a *B. subtilis* disome model[52]. After 2D classification in Relion 3.1[83], 82,276 particles representing collided disomes were selected for further processing. 3D classification and refinement in Relion resulted in a class of 19,230 particles displaying the density previously identified as corresponding to MutS2 SMR and KOW domains. This class was used for high-resolution refinement in CryoSPARC[84], resulting in a reconstruction with an overall resolution of 6.8 Å.

2.2.15 In vitro splitting assay

Purified versions (WT, SMR domain mutants, Walker A and Walker B mutants) of the MutS2 protein were added to purified disomes from *B. subtilis* in ten-fold excess in reaction buffer (50 mM HEPES/KOH pH 7.5, 75 mM KOAc, 5 mM $Mg(OAc)_2$, 1.2 mM DTT, 45 mM NH_4Cl, 4 mM $MgCl_2$, 1% glycerol, 1 mM $MnCl_2$) together with 1 mM ATP, 1 mM AMP-PNP, or no additional nucleotides and the mixture was incubated at 30 °C for 1 h. Samples were then applied to 10–50% continuous sucrose density gradients (50 mM HEPES/KOH pH 7.5, 100 mM KOAc, 5 mM $Mg(OAc)_2$, 1 mM DTT). The gradients were centrifuged in an SW40Ti rotor (Beckman Coulter) at 202,408 G for 150 min and

fractionated using a BioComp Gradient Station while UV absorption at 260 nm was recorded using a Triax Flow Cell FC-2.

2.3 Results

2.3.1 Different architectures of bacterial SMR domain proteins

SMR domain proteins recognize ribosome collisions and cleave mRNA in *S. cerevisiae* (Cue2), *C. elegans* (NONU-1), and *E. coli* (SmrB) during ribosome rescue[50,52,88]. This study was prompted by our observation that SMR domain proteins are broadly conserved in bacteria and cluster in three major clades with distinct domain architectures (Fig. 2.1 A,B). In *E. coli* and many other proteobacteria, the SMR domain is preceded by a relatively unstructured N-terminal extension, as observed in SmrB (21 kD). Our previous structural and biochemical studies revealed that conserved residues in a helix in this extension (the N-terminal hook) bind to the ribosomal protein uS2 and play a key role in recruiting SmrB to ribosomes[52].

In contrast, the architecture most commonly found in other bacterial phyla is more complex, typified by the MutS2 protein in *B. subtilis* (87 kD). From N- to C-terminus, this architecture contains the core/lever, clamp, P-loop ABC ATPase, KOW, and SMR domains (Fig. 2.1 B). Notably, although the core/lever, clamp, and ATPase domains take their names from the homologous MutS protein involved in DNA mismatch repair[89], the MutS2 architecture lacks two N-terminal domains found in MutS,

the MutSI (mismatch recognition) and MutSII (connector) domains. The absence of these two domains argues against MutS2 being involved in mismatch repair.

Finally, the third clade is the smallest, restricted to the Bacteroidetes lineage. SMR domain proteins in this clade only have an N-terminal KOW domain and C-terminal SMR domain (e.g., *C. baltica*, Fig. 2.1 B), occasionally with an IG-like domain in between the two. Notably, some KOW domains in bacteria are known to have ribosome binding activity; for example, the KOW domain of NusG binds to ribosomal protein uS10[90], raising the possibility that the KOW domain in these two architectures (MutS2-like and KOW-SMR) plays a role in recruiting SMR domain proteins to the ribosome.

Alignment of the SMR domains also revealed that residues previously implicated in mRNA cleavage are not equally conserved in these three clades. The DxH and GxG motifs in the SMR domain play a role in mRNA cleavage and RNA binding in *E. coli*[52], yeast[50], and plants[91]; these residues are highly conserved in SmrB proteins in proteobacteria and in the KOW-SMR protein in Bacteroidetes. In contrast, we identified several independent occasions where the DxH active site residues have been wholly or partly lost in the MutS2 clade. An alignment of the SMR domain from MutS2 in firmicutes is shown in Fig. 2.2. Many proteins have completely lost the DxH motif, whereas others such as *B. subtilis* MutS2 have the residues DLR which do not fully conform to the consensus DxH motif. In contrast, the GxG motif is highly conserved in firmicutes, as is the His residue just upstream (residue His743 in *B. subtilis* MutS2). These observations raise questions about whether SMR domains in the MutS2 clade retain the endonucleolytic activity observed in *E. coli* SmrB.

2.3.2 ΔmutS2 cells are hypersensitive to antibiotics that target ribosomes

To explore whether the MutS2 protein in *B. subtilis* plays a role in translation, we first examined the phenotype of a strain lacking this factor. *ΔmutS2* cells did not have a significant growth defect compared to wild-type cells on plates made with rich medium. However, cells lacking MutS2 are hypersensitive to several antibiotics that target the ribosome. On plates with chloramphenicol (CAM), tetracycline (TET), or erythromycin (ERY), the growth of the *ΔmutS2* strain is less robust than wild-type (Fig. 2.1 C). In contrast, the *ΔmutS2* strain is not sensitive to beta-lactam antibiotics (e.g., carbenicillin) that target cell wall synthesis (Fig 2.3). These results suggest that MutS2 plays a role in mediating the toxicity of antibiotics that perturb the elongation stage of protein synthesis.

2.3.3 MutS2 preferentially binds collided ribosomes

We next asked whether MutS2 associates with ribosomes *in vivo*. To facilitate the detection of MutS2, we ectopically expressed an N-terminally FLAG-tagged MutS2 construct from its native promoter in the *ΔmutS2* strain. We treated these cells with varying concentrations of CAM to ask how ribosome collisions affect MutS2 binding to ribosomes. As shown previously in yeast and *E. coli*, high concentrations of antibiotics that target the ribosome stall ribosomes quickly in place, whereas lower doses only stall some ribosomes, allowing others to continue elongating until they collide with the stalled ribosomes[41,52]. We used this strategy to ask if MutS2 binds preferentially to

collided ribosomes. In the untreated sample, MutS2 mostly is found in the light fractions of the sucrose gradient, although some portion is also found associated with monosomes and light polysomes, arguing that it can bind to ribosomes generally (Fig. 2.1 D). MutS2 is enriched in polysomes deeper in the gradient when cells were treated with a low dose of CAM (2 μg/mL), a concentration roughly equivalent to the minimum inhibitory concentration (MIC). Importantly, the enrichment of MutS2 in polysomes is lost in cells treated with much higher concentrations of CAM (200 μg/mL) (Fig. 2.1 D). We conclude that MutS2 weakly binds ribosomes in general and that its binding is enhanced by collisions, not merely by ribosome stalling.

We also asked whether MutS2 is preferentially recruited to nuclease-resistant disomes, a hallmark of collided ribosomes. Treatment of lysates with RNase A typically collapses most polysomes into monosomes, but when ribosomes have collided, RNase A cannot access the mRNA in the tight interface between them, thus leading to disome accumulation[42]. In untreated samples, polysomes collapsed into monosomes and MutS2 was mostly present in the lighter fractions (Fig. 2.1 E). However, in cells treated with 2 μg/mL CAM to induce collisions, small peaks corresponding to nuclease-resistant disomes and trisomes were identified; we observe that MutS2 is strongly enriched in those deeper fractions (Fig. 2.1 E). As expected, in samples treated with high concentrations of CAM, MutS2 was not enriched in the heavier fractions.

2.3.4 The structure of the KOW and SMR domains of MutS2 on collided ribosomes

The structure of MutS2 as a homodimer bound to collided ribosomes was previously visualized by cryo-electron microscopy by Cerullo *et al*. Although their structure reveals the overall arrangement of the lever, clamp, and ATPase domains of MutS2 on collided disomes, it does not provide insight into the positioning of the KOW and SMR domains in this interaction, nor does it reveal how collided ribosomes are specifically recognized. In order to further elucidate the mechanisms of MutS2 recruitment and activity, we reconstituted the complex *in vitro*. From an *in vitro* translation reaction of the MifM stalling construct in *B. subtilis* lysates, we purified disomes from a sucrose density gradient as described previously[52,92]. We purified recombinant *B. subtilis* MutS2 (Fig. 2.4 A) and observed by size-exclusion chromatography that it exists as an oligomer (Fig. 2.4 B) as reported for MutS2 from other bacteria[93,94]. A ten-fold excess of MutS2 protein was added to the disomes and the reaction was incubated in the presence of AMP-PNP. The sample was then vitrified and subjected to cryo-EM and single-particle analysis.

We observe two major classes of collided disomes: one with only mRNA density in the inter-ribosomal space and another with an additional density next to the mRNA (Figs. 2.5 A,B and 2.6). The latter class also contains additional density next to uS10 on both the stalled and the collided ribosomes. By local refinement of the experimental data and rigid body-fitting of a model of MutS2 generated in Alphafold2[85], we identified these extra densities as the SMR and KOW domains, respectively (Fig. 2.5 B). As described below, we were not able to visualize the N-terminal domains seen in the previous structure (lever, clamp, and ATPase).

The overall architecture of the collided disome bound by the MutS2 KOW and SMR domains is shown in Fig. 2.5 C. Only one SMR domain is visible, next to the mRNA in the inter-ribosomal space, interacting with both ribosomes (Fig. 2.5 D). In this position, the region of the SMR domain containing the DLR and GxG residues is oriented towards the mRNA, suggesting a specific interaction as we previously observed for SmrB in *E. coli*[52] (Fig. 2.5 F,G). On the stalled ribosome, the SMR domain interacts with uS11 and uS7, as does SmrB; on the collided ribosome, the SMR domain is positioned next to uS3.

The two KOW domains bind to ribosome protein uS10 in a manner that is highly similar to the KOW domain of NusG, an *E. coli* protein involved in transcription-translation coupling[90]. The KOW domain on the collided ribosome is connected to the SMR domain by partial density, consistent with a flexible loop joining them, arguing that these domains derive from the same MutS2 monomer. The KOW domain on the stalled ribosome is part of the second MutS2 in the homodimer whose other domains are not resolved. The position of the two KOW domains is compatible with the position of the coiled-coil domains in MutS2 in the previous structure[63]. Indeed, partial density for the KOW domain on the collided ribosome is seen linked to the N-terminal domains in the electron density maps of the earlier study though it was not discussed there[63]. We conclude that no structural rearrangements would be required to link the density of the N-terminal domains in the previous structure with the C-terminal KOW and SMR domains reported here (Fig. 2.7 A–C).

Finally, although the SMR domains of both MutS2 and SmrB recognize composite binding sites formed between the collided ribosomes near the bridging mRNA, the orientation of the SMR domain is very different in the two complexes from *B. subtilis* and *E. coli*. This difference in the SMR domain orientation may arise from constraints imposed by additional interactions of the N-terminal hook of SmrB with uS2 and by the MutS2 KOW domain with uS10. As a result, compared to SmrB, the SMR domain of MutS2 is rotated around the mRNA by ~120° (Fig. 2.5 E). Together with the lack of strong amino acid conservation, this finding raises the question as to whether the SMR domain of MutS2 possesses the same endonucleolytic activity as SmrB[52].

2.3.5 Attempts to reconcile the differences in the structures

Not only were different MutS2 domains resolved in our structure and the previous one by Cerullo *et al*, there are also discrepancies in the conformation and composition of the ribosome. Here, only in disomes where both ribosomes adopt a non-rotated (or classical) conformation do we find density corresponding to the SMR domain, despite the presence of collided disomes in other states in our dataset. In contrast, in the Cerullo structure, the collided ribosome appears in a rotated (or hybrid) conformation. In addition, there are differences in the ribosome proteins present at the disome interface: bS21 is missing in the stalled ribosome in our structure (Fig. 2.7 F,G) where it was previously observed, and uS2 is clearly present on both the stalled and collided ribosomes in our structure (Figs. 2.5 C and 2.7 E), although it was previously missing from the stalled ribosome.

Thinking that these discrepancies might arise from differences in how the complexes were prepared, we isolated native MutS2-disome complexes from *B. subtilis* cells expressing FLAG-tagged MutS2 (containing the Walker B mutation) by affinity purification. Analysis of this native complex revealed a cryo-EM reconstruction containing extra densities corresponding to the SMR and KOW domains (Fig. 2.7 H), albeit at a lower resolution than the *in vitro* complex described above, but without density corresponding to the N-terminal domains. Likewise, we observed clear density for uS2 on the stalled ribosome and at most partial density in the binding pocket of bS21 (Fig. 2.7 I). The collided ribosome, however, assumes the same rotated conformation described previously[63], meaning that binding of the SMR domain is compatible with this ribosome conformation. We speculate that MutS2 may bind collided ribosomes in a non-rotated state (as we observed *in vitro*) followed by a transition to a rotated state *in vivo* or during the purification procedure. These experiments on the native complex suggest that the discrepancies in the ribosome protein composition and MutS2 structures reported here and by Cerullo *et al* are not due to the formation of the complex *in vivo* or *in vitro*.

One interpretation is that MutS2 interacts with collided disomes in two states, either through the KOW and the SMR domains or through the KOW and N-terminal domains (lever, clamp, ATPase). Perhaps the SMR and KOW domains facilitate disome recognition and MutS2 recruitment, and when the ATPase domain binds in a pre-splitting conformation, the interactions with the SMR domain become dispensable and thus no longer visible by cryo-EM.

2.3.6 MutS2 releases truncated proteins from stalled ribosomes but does not affect mRNA levels

To study the activity of MutS2 *in vivo*, we designed reporter constructs that allow us to follow the translation of a problematic mRNA in *B. subtilis* (Fig. 2.8 A). Each reporter contains an in-frame fusion of NanoLuc to the bleomycin resistance protein (BleR). We created two control constructs, one with a stop codon between the genes that produces NanoLuc alone (Stop) and a second without any stalling motif (Non-stall) that produces the full-length fusion protein. In a third construct, we inserted the 31-residue ApdA stalling motif between NanoLuc and BleR (ApdA). This arrest peptide from *A. japonica* arrests elongating *B. subtilis* ribosomes by inhibiting peptidyl transfer[5].

To confirm that ribosome stalling at ApdA triggers downstream rescue pathways, we performed a western blot using antibodies against NanoLuc. A strong band corresponding to full-length protein is observed for the Non-stall control and loss of MutS2 did not affect this reporter, as expected (Fig. 2.8 B). In contrast, there is significantly less full-length protein for the ApdA reporter because stalling lowers the protein output. Moreover, the ApdA reporter generates a truncated protein that is slightly larger than the NanoLuc produced from the Stop control, consistent with the translation of the additional ApdA sequence prior to ribosome stalling. Importantly, the loss of MutS2 resulted in a substantial decrease in the amount of truncated reporter protein from the ApdA reporter (Fig. 2.8 B). These results are consistent with a model in

which MutS2 rescues ribosomes stalled in the middle of an open reading frame (ORF) thus releasing truncated protein products.

In addition, we analyzed the activity of MutS2 on the reporter mRNA using northern probes specific for the 5'- or 3'-ends (Fig. 2.8 C). With the 5'-probe, we see primarily full-length mRNA from the Non-stall reporter. Remarkably, there appear to be similar levels of full-length mRNA from the ApdA reporter as well, in stark contrast to our previous observation in *E. coli* that the presence of a strong arrest peptide dramatically lowers full-length reporter mRNA levels[52]. This finding suggests that unlike in *E. coli*, where ribosome stalling targets transcripts for decay by SmrB nuclease activity, ribosome stalling does not target the reporter mRNA for decay in *B. subtilis*. With the 3'-probe, again we see that full-length mRNA levels are similar with or without the ApdA stalling sequence. With this probe, we also detect a decay intermediate from the ApdA reporter corresponding to the mRNA fragment downstream of the stall site; importantly, loss of MutS2 does not affect the level of this fragment, suggesting that MutS2 is not responsible for its production. We speculate that the truncated band arises from the degradation of the upstream mRNA by the 5'–3' exonucleases until they are blocked by the stalled ribosome, yielding a stable, downstream fragment[95,96]. Taken together, these data show that MutS2 generates a truncated protein product from ribosomes stalled in the middle of an ORF but does not affect mRNA levels, suggesting that, unlike SmrB, it may indeed lack nuclease activity.

2.3.7 Ala-tailing by RqcH depends on MutS2

We envisioned that MutS2 might release truncated proteins from stalled ribosomes in two different ways, depending on the activity of the protein; these possibilities are not mutually exclusive. First, if MutS2 were to cleave the mRNA on collided ribosomes, then upstream ribosomes would arrest at the newly formed 3'-end and be rescued by tmRNA, leading to the release of a truncated protein with C-terminal SsrA tags encoded by tmRNA during the rescue process. Typically, SsrA-tagged proteins are rapidly degraded by the ClpXP protease[97]. If the tmRNA system is overwhelmed, however, a backup system involving ArfA in *E. coli* or BrfA in *B. subtilis* typically releases the nascent peptide without adding a degron tag[23,33,56]. In *E. coli*, we previously observed that cells lacking tmRNA generate far higher levels of truncated protein products from a stalling reporter because the ArfA-released (and therefore untagged) protein products are stable relative to those that were tagged by tmRNA[52]. We find that in *B. subtilis* cells in which the tmRNA pathway was inactivated by deletion of its protein partner SmpB, there is no difference in the level of truncated protein produced compared to the wild-type cells (Fig. 2.8 D); thus, there is no major role for the tmRNA system in resolving the stalled ribosomes on the ApdA reporter. This finding is consistent with the lack of evidence that MutS2 cleaves the reporter mRNA to generate a prototypical nonstop message substrate for tmRNA/SmpB.

A second possible mechanism of action is that the ATPase domain of MutS2 splits the stalled ribosome into subunits, freeing the 30 S subunit but yielding a 50 S subunit with peptidyl-tRNA trapped on it, akin to the activity of RQT in eukaryotic systems[75]. It has been shown that in *B. subtilis* (as in eukaryotes) the 50S-peptidyl-tRNA

complex is a substrate for the RQC factor RqcH which adds several Ala residues to the C-terminus of the nascent polypeptide and targets the protein for degradation by ClpXP[57,59–61]. In this case, the expectation would be that deletion of RqcH should stabilize truncated proteins produced by this pathway because they would not be Ala-tailed[57]. Indeed, we observe higher levels of truncated protein from the reporter construct in the absence of RqcH (Fig. 2.8 D), consistent with the model proposed by Cerullo *et al* in which MutS2 splits ribosomes into subunits that are then acted on by RqcH to target the nascent peptide for degradation[63].

To further characterize the truncated protein, we used mass spectrometry to identify C-terminal fragments to detect whether SsrA-tag or Ala-tails were added during the rescue process. We grew cells with bortezomib (an inhibitor of ClpXP) to prevent degradation of the truncated proteins and immunoprecipitated the ApdA reporter protein from wild-type, *ΔmutS2*, and *ΔrqcH* strains. We then digested the protein with lysyl endopeptidase and subjected the resulting peptides to liquid chromatography with tandem mass spectrometry (LC-MS/MS). Ribosomes stall near the end of the ApdA sequence at the RAPP motif with the first Pro codon in the P site and the second Pro codon in the A site[5]. We observed abundant peptides in all three strains ending in RAP (Fig. 2.8 E). These represent proteins unmodified by tmRNA or RqcH possibly arising from peptides released from the 50 S after splitting (without Ala-tails) or nascent peptides on 70 S ribosomes released from tRNA during sample preparation. More interestingly, we observe peptides with alanine tails added at the site of the stall (after RAP). These peptides are only observed in the wild-type strain. Deletion of RqcH leads to

loss of Ala-tailing, as expected, and likewise, deletion of MutS2 also leads to loss of Ala-tailing (Fig. 2.8 E). These findings are consistent with a model wherein MutS2 activity is upstream of Ala-tailing by RqcH in vivo. Indeed, based on their observations of loss of Ala-tagging in strains lacking MutS2, Cerullo *et al* proposed renaming MutS2 as RqcU (RQC-upstream factor).

We also observed proteins that had been tagged by tmRNA. These peptides were less abundant than those released at the stall site (ending in RAP) or those with Ala-tails, although with the challenges in mass spectrometry in detecting various peptides we cannot make any strong quantitative conclusions. The tmRNA tag is added to peptides right at the stall site after the RAP motif (Fig. 2.8 F) as well as at a second site after the Gly residue four residues upstream. In both cases, the number of tmRNA-tagged peptides was not reduced in samples prepared from cells lacking MutS2, arguing that MutS2 is not functioning upstream of tmRNA tagging at either site. We argue that tmRNA tagging arises from mRNA decay pathways unrelated to MutS2 in *B. subtilis*. These data are in stark contrast to our earlier observations in *E. coli* where tmRNA-tagged products arising from upstream of the stall site disappear when SmrB is deleted (PMID: 35264790). Taken together, these data are consistent with a role for MutS2 in splitting the downstream ribosome into subunits (leading to Ala-tailing by RqcH) but do not provide evidence in support of mRNA cleavage by MutS2.

2.3.8 The KOW and SMR domains promote MutS2 binding to collided ribosomes

With insights from the cryo-EM structure, we next made a series of MutS2 mutations to determine how each domain contributes to binding collided ribosomes in vivo. Mutant FLAG-tagged MutS2 constructs were expressed from an ectopic site in the *ΔmutS2* strain; the expression levels of all the mutants were found to be roughly equivalent (Fig 2.9). We treated cultures with a low dose of CAM to induce collisions and performed western blots using anti-FLAG antibodies to follow MutS2 sedimentation across sucrose gradients.

Given that our structure revealed that the KOW domain binds to ribosomal protein uS10, we made several Ala mutations in a single construct designed to perturb the binding interface (KOWmut), including Q668A, I671A, L672A, and K673A. These surface-exposed residues lie in a loop corresponding to the conserved F165 in the KOW domain of NusG that is critical for ribosome binding[90]. As expected, binding of the KOW-mut protein is reduced compared to the wild-type (Fig. 2.10 A); there is more protein in the first fractions and less bound to ribosomes deeper in the gradient.

The fact that the SMR domain is buried between the collided ribosomes suggests that it may specifically sense collisions through the recognition of a distinct, composite binding interface. Indeed, deletion of the SMR domain (ΔSMR) through truncation after residue 701 dramatically reduces MutS2 binding to ribosomes (Fig. 2.10 A). We also made mutations to conserved residues in the SMR domain likely to be involved in RNA binding, independently changing D711LR to ALA and mutating the conserved His just upstream of the GxG motif (H743A). Both the ALA mutant and the H743A mutant show dramatic reductions in binding to colliding ribosomes (Fig. 2.10 A). In contrast, we found

that mutation of the Walker B motif (E416A) in the ATPase domain had little or no effect; this mutant protein still shifts deep into polysomes when collisions are induced (Fig. 2.10 A). These results with the MutS2 mutants show that, consistent with our cryo-EM structure, the KOW and especially the SMR domain promote MutS2 binding to collided ribosomes.

2.3.9 The ABC ATPase domain is critical for MutS2 function

To determine the effect of these mutations on the activity of MutS2, we introduced the ApdA stalling reporter into strains carrying the MutS2 mutants. We added bortezomib to cultures to prevent degradation of the truncated protein and performed western blots against NanoLuc, the upstream part of the stalling reporter. In wild-type cells, there is a strong band corresponding to the truncated reporter that is stabilized relative to the full-length protein by the addition of bortezomib (Fig. 2.10 B) compared to untreated samples (Fig. 2.8 B). There is also a band just below the major band that is not dependent on MutS2; in the *ΔmutS2* strain, only the top band decreases (TR), not the lower band (*). When a Flag-tagged copy of wild-type MutS2 is added to complement the deletion, the upper band, TR, is rescued to wild-type levels, indicating that the Flag-tag does not impact MutS2 activity.

The Walker B mutant yields little or no truncated MutS2 product (the TR band), similar to the complete knockout strain, *ΔmutS2* (Fig. 2.10 B); these data indicate that inhibiting ATP hydrolysis abrogates MutS2 activity. In contrast, mutation of the KOW domain (KOW-mut) or the SMR domain (ΔSMR, ALA, H743A) yielded an intermediate

phenotype, where we saw some reduction in the level of the upper band, but not a complete loss of MutS2 product. This loss of activity is likely due to the reduction in binding observed in Fig. 2.10 A.

We also tested the effects of MutS2 mutations on the ability of cells to survive on plates with the collision-inducing antibiotic erythromycin (ERY). Just as *B. subtilis* cells lacking MutS2 are sensitive to ERY, so too are cells expressing the Walker B mutant (Fig. 2.10 C). In contrast, cells expressing the KOW-mut or mutations in the SMR domain showed only very modest sensitivity to ERY. These results show that the ATPase domain of MutS2 is associated with its most critical functional domain.

2.3.10 MutS2 splits disomes into ribosome subunits in vitro

We reconstituted disome splitting *in vitro*, purifying *B. subtilis* disomes from an *in vitro* translation reaction and combining them with purified wild-type or mutant MutS2. The reactions were then fractionated on a sucrose gradient in order to analyze the relative abundance of the remaining disomes, monosomes, and ribosome subunits, in order to determine the splitting efficiency.

When incubating the collided disomes with wild-type MutS2 in the presence of ATP, we generally observed a marked decrease in the disome peak compared to a control experiment in the absence of ATP. At the same time, we observed an increase in peaks corresponding to ribosomal subunits and monosomes, indicating disome splitting activity by MutS2 (Fig. 2.11 A, red). In these experiments, the contribution of the disome peak area to the total for all ribosomal fractions decreased by at least 40%. However,

when ATP was substituted with the non-hydrolyzable analog AMPPNP, no such decrease was observed, confirming that ATP hydrolysis is required for MutS2 splitting activity and that ATP binding alone is not sufficient (Fig. 2.11 A). We also found that the Walker A and Walker B mutants of MutS2 fail to split the disomes, even in the presence of ATP (Fig. 2.11 B); these data establish that ATP binding followed by hydrolysis by the MutS2 ATPase domain is required for efficient dissociation of disomes *in vitro*. In contrast, repeating the experiment with the MutS2 ALA mutant, which disrupts the DLR motif of the SMR domain, yielded similar splitting activity when comparing the SMR domain mutant with wild-type MutS2 (Fig. 2.12). These data further argue that these residues in the SMR domain of MutS2 are not essential for disome splitting and that MutS2 does not carry out an endonuclease function.

2.3.11 Nonstop reporter mRNA is not preferentially decayed in B. subtilis

Observing the lack of cleavage in RQC in B. subtilis made us wonder about the mRNA stability of nonstop messages in *B. subtilis* as well. As discussed in the introduction of this chapter, in *E. coli*, nonstop messages are rescued by tmRNA in trans-translation and are much less stable than full length mRNAs[20,21]. We wondered if this is also true in *B. subtilis*.

To study trans-translation *in vivo*, we designed reporter constructs to follow the rescue of ribosomes stalled on nonstop transcripts. The reporter consists of a nano-luciferase gene (NanoLuc) which also contains a N-terminal Strep tag. The control reporter (Stop) contains a stop codon at the end of the NanoLuc ORF and the nonstop

reporter (NonStop) does not contain a stop codon (Fig 2.13 A). To confirm what has previously been reported with nonstop messages, we expressed these reporters ectopically in both wild-type (WT) and tmRNAΔ strains in *E. coli* and *B. subtilis* and visualized reporter protein levels by western blot using antibodies against NanoLuc. The Stop reporter protein was detected at similar levels in both strains in *E. coli* and *B. subtilis*, as expected (Fig 2.13 B). However, NonStop reporter protein could not be detected in WT cells in both *E. coli* and *B. subtilis*; as previously shown, the tmRNA pathway targets the NonStop reporter for degradation in WT cells in both bacterial species. Without tmRNA, the nonstop protein accumulates as it is released by the ArfA/BrfA systems without tagging (Fig 2.13 B). Together these data confirm what has been previously shown for degradation of the nascent peptide through trans-translation by tmRNA in both *E. coli* and *B. subtilis*.

To analyze the effects of trans-translation on the NonStop reporter mRNA, we used a probe specific to the 5' end of the reporter for northern blotting. In *E. coli*, the NonStop reporter RNA was not detected in WT cells while the Stop reporter is stably expressed (Fig 2.13 C) which corroborates what has been reported previously that nonstop messages are decayed rapidly in *E. coli*. In cells lacking tmRNA, the full-length NonStop reporter mRNA was detected (Fig 2.13 C) indicating that tmRNA plays an essential role for targeting nonstop messages for decay in *E. coli*.

Although the effect of tmRNA on nonstop mRNAs has been shown in *E. coli*, this has not been explored in *B. subtilis*. When the NonStop reporter mRNA is expressed in WT *B. subtilis* cells, the levels of reporter mRNA is equivalent to the Stop reporter RNA

(Fig 2.13 C). This starkly contrasts the results from *E. coli*. In tmRNAΔ *B. subtilis* cells, the levels of reporter RNA for the NonStop and Stop constructs are also equivalent (Fig 2.13 C). These results clearly show that in *B. subtilis*, nonstop mRNAs are not preferentially decayed by the trans-translation rescue pathway.

Previous work by Karzai and others showed that in *E. coli*, nonstop messages are decayed by RNase R which is recruited by tmRNA[20,21]. To investigate the role of exonucleases on nonstop message decay in *E. coli* and *B. subtilis*, we introduced the NonStop reporter construct into cells lacking various 3'-5' exonucleases. In *E. coli*, deleting RNase R, RNase II, or PNPase does not stabilize the NonStop reporter protein (Fig 2.13 B). In *B. subtilis*, deletion of RNase R or PNPase also does not stabilize the NonStop reporter protein (Fig 2.13 B). These results do not mean that the RNases are not involved in decaying nonstop mRNAs because there could be redundancy or compensatory mechanisms that we are not able to parse out with single knockouts. There is also the possibility that the reporter construct used in the Karzai papers were targets of RNase R, but because we are using a different construct, our NonStop reporter may not be.

In *E. coli*, deletion of RNase R did not result in stabilization of NonStop reporter mRNA; NonStop reporter mRNA was stabilized only in the tmRNAΔ strain (Fig 2.13 C). In *B. subtilis* since the NonStop reporter mRNA is not preferentially decayed as in *E. coli*, we did not expect to see a difference by deleting exonucleases. That is exactly what we observed. Deletion of RNase R or PNPase had no effect on the NonStop reporter mRNA as compared to WT cells in *B. subtilis* (Fig 2.13 C). The lack of an mRNA decay phenotype

with trans-translation in *B. subtilis* mirrors the lack of mRNA decay in RQC in *B. subtilis* as well.

2.4 Discussion

The data presented here support a model in which *B. subtilis* MutS2 promotes the rescue of stalled ribosomes in a dramatically different manner from *E. coli* SmrB (Fig. 2.14). Although both proteins contain an SMR domain that recognizes the interface formed by two colliding ribosomes, helping to recruit them to their disome substrate, the biochemical activities of the two proteins are distinct. The SMR domain in SmrB functions as an endonuclease, cleaving mRNA between the collided ribosomes, allowing upstream ribosomes to translate to the newly formed 3'-end, where they are rapidly rescued by tmRNA. After canonical release and recycling on the tmRNA template, the tag encoded by tmRNA leads to degradation of the nascent peptide by proteases. In contrast, the SMR domain in *B. subtilis* MutS2 is not an active nuclease, nor does it target ribosomes for rescue by tmRNA. Instead, the ATPase domain of MutS2 splits the stalled ribosomes into subunits, freeing the 30 S subunit as well as a 50 S subunit bound to peptidyl-tRNA. RqcH then facilitates the non-templated addition of Ala residues to the C-terminus of the nascent peptide, and after the peptide is released from the tRNA through an unknown mechanism, the Ala-tail targets it for degradation by proteases. Through these distinct mechanisms, both SmrB and MutS2 trigger pathways that recycle the stalled ribosomes and degrade the aborted nascent polypeptides.

In this study, we clarify MutS2's mechanism of action in recognizing collided ribosomes in *B. subtilis*. Ribosome collisions are present in diverse bacteria and share common features. In *E. coli* and in *B. subtilis*, the SMR domain plays a role in recruiting both SmrB and MutS2 to collided ribosomes, recognizing the similar composite binding site formed between the two ribosomes. In both cases, residues in the DxH/DLR and HGxG motifs are oriented towards the mRNA. In the case of SmrB, the DLH residues are involved in catalysis; in the case of MutS2, our data suggest that the DLR and HGxG sequences are required for high affinity binding to ribosomes but not for endonucleolytic cleavage. We note that the sucrose gradient sedimentation binding assay is a stringent test as evidenced by the fact that SMR domain mutants that fail to bind robustly still retain partial rescue activity. Ribosome binding is likely aided by auxiliary interactions of SmrB and MutS2 with the periphery of the collision interface, at sites that are accessible on all ribosomes, not only collided ones. For example, the interactions between the KOW domain of MutS2 and uS10 may be sufficient for partial activity even without the SMR domain. Most notably, as revealed by cryo-EM structures, the orientations of the SMR domains of SmrB and MutS2 are completely different, consistent with the difference in terms of catalytic activity of the two proteins.

Apparently, although SMR domains act as conserved ribosome collisions sensors in bacteria, not all have nuclease activity. We do not see any evidence that MutS2 targets mRNAs encoding stalling sequences for degradation as SmrB does so effectively in *E. coli*. Consistent with this, although the DxH residues associated with SmrB endonuclease activity in proteobacteria are also conserved in Bacteroidetes proteins

with the KOW-SMR architecture, they are only rarely present in the proteins with the MutS2 architecture. Substitution of the histidine in the DxH motif required for metal-independent catalysis appears to be a repeated theme throughout the SMR family, occurring several times in various lineages. The SmrA proteins in gammaproteobacteria, for example, which are paralogs of SmrB, wholly lack the residues necessary for nuclease activity. In plants, SMR domains display a diversity of active sites, with some retaining the DxH, others containing the same DxR motif reported here for MutS2, and still others with further substitutions of these residues[88].

Based on the growing evidence for the role of SMR domains in sensing ribosome collisions, we propose that SMR domain proteins participate in at least two pathways. The active versions, like SmrB, Cue2, and Nonu-1, work via mRNA cleavage at collisions. In bacteria, cleavage leads to ribosome rescue by the tmRNA pathway; in eukaryotes, the active SMR versions likely function along with the exosomal mRNA degradation system conserved in the archaeoeukaryotic lineage. In contrast, the inactive versions, like MutS2, are likely to depend on ribosome-splitting pathways coupled with the ancient RqcH/Rqc2 pathway that was present in the last universal common ancestor. While MutS2 carries its own ABC ATPase domain, critical for ribosome splitting, in eukaryotes the inactive SMR domains could function along with related but distinct ribosome-splitting enzymes of the translation factor ABC ATPase clade (e.g., Rli1 in yeast and ABCE1 in humans). Thus, the SMR domains parallel the evolution of the RNase H-fold release factor (eRF1) family[98], which also features both catalytically active versions

involved in the release of the polypeptide from the tRNA (e.g., eRF1) and inactive versions that separate ribosomal subunits (e.g., Dom34 in yeast and PELO in humans).

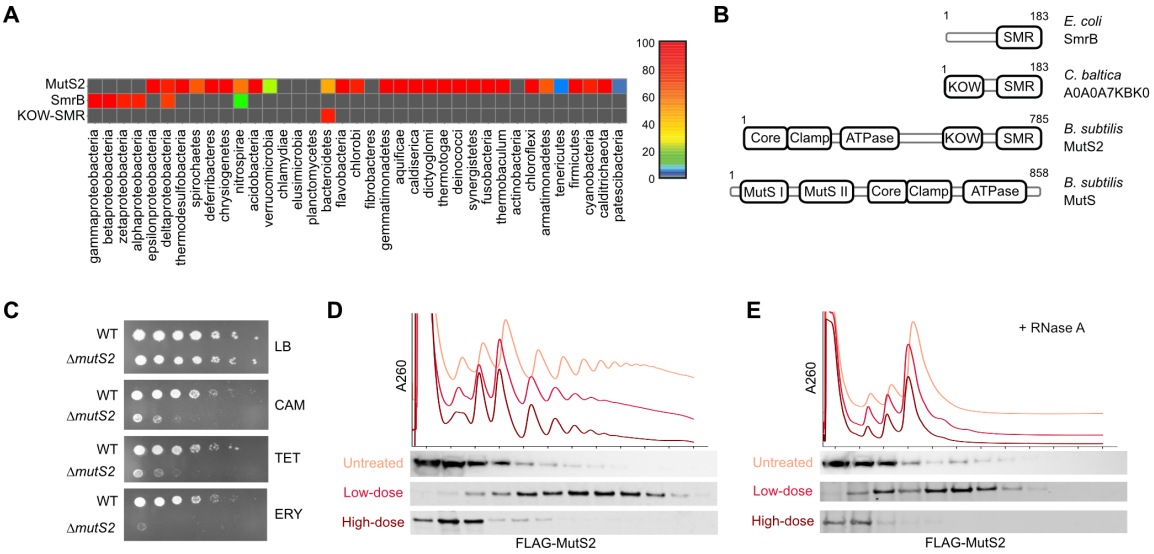
A
MutS2
SmrB
KOW-SMR
gammaproteobacteria
betaproteobacteria
zetaproteobacteria
alphaproteobacteria
epsilonproteobacteria
deltaproteobacteria
thermodesulfobacteria
spirochaetes
deferribacteres
chrysiogenetes
nitrospirae
acidobacteria
verrucomicrobia
chlamydiae
elusimicrobia
planctomycetes
bacteroidetes
flavobacteria
chlorobi
fibrobacteres
gemmatimonadetes
aquificae
caldiserica
dictyoglomi
thermotogae
deinococci
synergistetes
fusobacteria
thermobaculum
actinobacteria
chloroflexi
armatimonadetes
tenericutes
firmicutes
cyanobacteria
calditrichaeota
patescibacteria
100
80
60
40
20
0
B
1
183
SMR
E. coli
SmrB
KOW
C. baltica
A0A0A7KBK0
785
Core
Clamp
ATPase
B. subtilis
MutS2
858
MutS I
MutS II
MutS
C
WT
ΔmutS2
LB
CAM
TET
ERY
D
A260
Untreated
Low-dose
High-dose
FLAG-MutS2
E
+ RNase A
A260
Untreated
Low-dose
High-dose
FLAG-MutS2

Figure 2.1 MutS2, an SMR domain protein in *B. subtilis*, binds collided ribosomes. (A) Heatmap showing the percentage of genomes in each bacterial phylum encoding an SMR domain protein. (B) Domain organization of three representative bacterial SMR domain proteins and the related DNA mismatch repair factor MutS. (C) Spotting assay showing *ΔmutS2* cells are hypersensitive to chloramphenicol (CAM) (1 μg/mL), tetracycline (TET) (2 μg/mL), and erythromycin (ERY) (0.08 μg/mL). (D) Low doses of CAM induce collisions whereas high doses stall ribosomes without inducing collisions. Following treatment with low-dose (2 μg/mL) and high-dose (200 μg/mL) CAM, the distribution of FLAG-MutS2 was determined by fractionation over sucrose gradients and detection with an anti-FLAG antibody. (E) Lysates from cells with and without CAM were treated with RNase A, fractionated over sucrose gradients, and the binding of FLAG-MutS2 to nuclease-resistant disomes was detected with an anti-FLAG antibody.

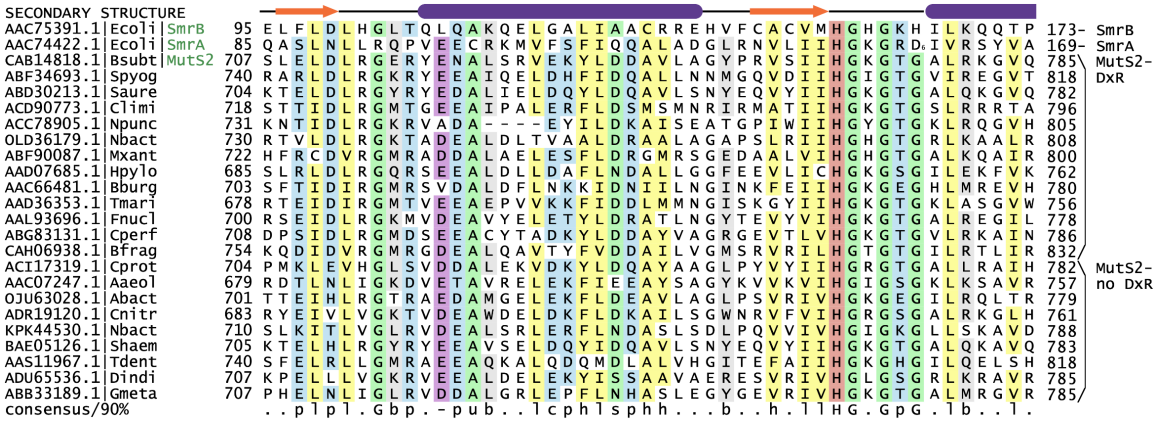
SECONDARY STRUCTURE
AAC75391.1|Ecoli|SmrB 95 E L F L D L H G L T Q L Q A K Q E L G A L I A A C R R E H V F C A C V M H G H G K H I L K Q Q T P 173- SmrB
AAC74422.1|Ecoli|SmrA 85 Q A S L N L L R Q P V E E C R K M V F S F I Q Q A L A D G L R N V L I I H G K G R D I V R S Y V A 169- SmrA
CAB14818.1|Bsubt|MutS2 707 S L E L D L R G E R Y E N A L S R V E K Y L D D A V L A G Y P R V S I I H G K G T G A L R K G V Q 785 MutS2-
ABF34693.1|Spyog 740 R A R L D L R G K R Y E E A I Q E L D H F I D Q A L L N N M G Q V D I I H G I G T G V I R E G V T 818 DxR
ABD30213.1|Saure 704 K T E L D L R G Y R Y E D A L I E L D Q Y L D Q A V L S N Y E Q V Y I I H G K G T G A L Q K G V Q 782
ACD90773.1|Climi 718 S T T I D L R G M T G E E A I P A L E R F L D S M S M N R I R M A T I I H G K G T G S L R R R T A 796
ACC78905.1|Npunc 731 K N T I D L R G K R V A D A - - - - E Y I L D K A I S E A T G P I W I I H G Y G T G K L R Q G V H 805
OLD36179.1|Nbact 730 R T V L D L R G K T A D E A L D L T V A A L D R A A L A G A P S L R I I H G H G T G R L K A A L R 808
ABF90087.1|Mxant 722 H F R C D V R G M R A D D A L A E L E S F L D R G M R S G E D A A L V I H G H G T G A L K Q A I R 800
AAD07685.1|Hpylo 685 S L R L D L R G Q R S E E A L D L L D A F L N D A L L G G F E E V L I C H G K G S G I L E K F V K 762
AAC66481.1|Bburg 703 S F T I D I R G M R S V D A L D F L N K K I D N I I L N G I N K F E I I H G K G E G H L M R E V H 780
AAD36353.1|Tmari 678 R T E I D I R G M T V E E A E P V V K K F I D D L M M N G I S K G Y I I H G K G T G K L A S G V W 756
AAL93696.1|Fnucl 700 R S E I D L R G K M V D E A V Y E L E T Y L D R A T L N G Y T E V Y V I H G K G T G A L R E G I L 778
ABG83131.1|Cperf 708 D P S I D L R G M D S E E A C Y T A D K Y L D D A Y V A G R G E V T L V H G K G T G V L R K A I N 786
CAH06938.1|Bfrag 754 K Q D I D V R G M R G D E A L Q A V T Y F V D D A I L V G M S R V R I L H G T G T G I L R T L I R 832
ACI17319.1|Cprot 704 P M K L E V H G L S V D D A L E K V D K Y L D Q A Y A A G L P Y V Y I I H G R G T G A L L R A I H 782 MutS2-
AAC07247.1|Aaeol 679 R D T L N L I G K D V E T A V R E L E K F I E E A Y S A G Y K V V K V I H G I G S G K L K S A V R 757 no DxR
OJU63028.1|Abact 701 T T E I H L R G T R A E D A M G E L E K F L D E A V L A G L P S V R I V H G K G E G I L R Q L T R 779
ADR19120.1|Cnitr 683 R Y E I V L V G K T V D E A W D E L D K F L D K A I L S G W N R V F V I H G R G S G A L R K G L H 761
KPK44530.1|Nbact 710 S L K I T L V G L R V D E A L S R L E R F L N D A S L S D L P Q V V I V H G I G K G L L S K A V D 788
BAE05126.1|Shaem 705 K T E L H L R G Y R Y E E A V S E L D Q Y I D Q A V L S N Y E Q V Y I I H G K G T G A L Q K A V Q 783
AAS11967.1|Tdent 740 S F E L R L L G M R A E E A Q K A L Q D Q M D L A L V H G I T E F A I I H G K G H G I L Q E L S H 818
ADU65536.1|Dindi 707 K P E L L L V G K R V E E A L D E L E K Y I S S A A V A E R E S V R I V H G L G S G R L K R A V R 785
ABB33189.1|Gmeta 707 P H E L N L I G L R V D D A L G R L E P F L N H A S L E G Y G E V R I V H G K G T G A L M R G V R 785
consensus/90% . . p l p l . G b p . - p u b . . l c p h l s p h h . . . b . . h . l l H G . G p G . l b . . l .

Figure 2.2 Multiple alignment of the conserved residues in the SMR domains from different bacteria. Columns in the alignment are shaded and labeled according to biochemical character: −, negatively charged in purple; c, charged in blue; h, hydrophobic in yellow; p, polar in blue; l, aliphatic in yellow; b, big in gray; s, small in green; u, tiny in green; G, glycine in green; H, histidine in red. Sequences are labeled with NCBI accession number and organism abbreviation. Secondary structure provided at top of alignment. Numbers to left and right of alignment denote positioning of the region.

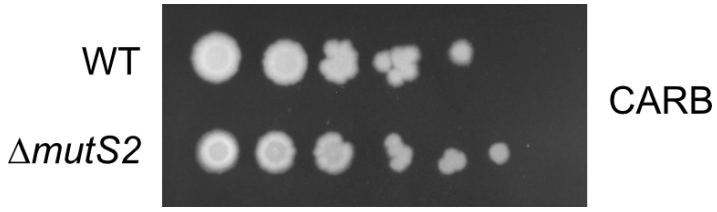
WT
ΔmutS2
CARB

Figure 2.3 Spotting assay showing that *ΔmutS2* cells are not hypersensitive to carbenicillin (0.05 μg/mL).

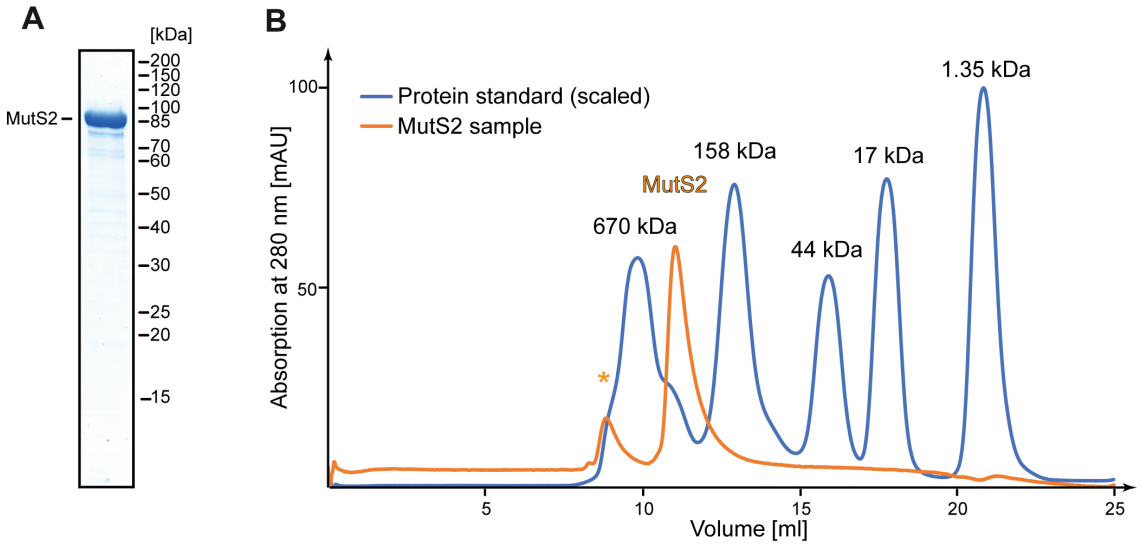
A
[kDa]
MutS2
200
150
120
100
85
70
60
50
40
30
25
20
15
B
Protein standard (scaled)
MutS2 sample
Absorption at 280 nm [mAU]
100
50
670 kDa
158 kDa
MutS2
44 kDa
17 kDa
1.35 kDa
*
5
10
15
20
25
Volume [ml]

Figure 2.4 MutS2 purification as an oligomer. (A) Purified sample of *B. subtilis* MutS2 used for reconstitution experiments, shown on a Coomassie-stained 10% Nu-PAGE gel. The expected apparent molecular weight of MutS2 is approximately 87 kDa. (B) Chromatograms of size-exclusion chromatography with the purified MutS2 sample (orange) and a protein size standard (blue) consisting of Thyroglobulin (bovine, 670 kDA), g-globulin (bovine, 158 kDa), Ovalbumin (chicken, 44 kDa), Myoglobin (horse, 17 kDa), and Vitamin B12 (1,35 kDa). Samples were analyzed on a Superdex 200 increase 10/300 GL column. Results indicate a single purified MutS2 complex of a size between 158 kDa and 670 kDa, consistent with a dimer or tetramer.

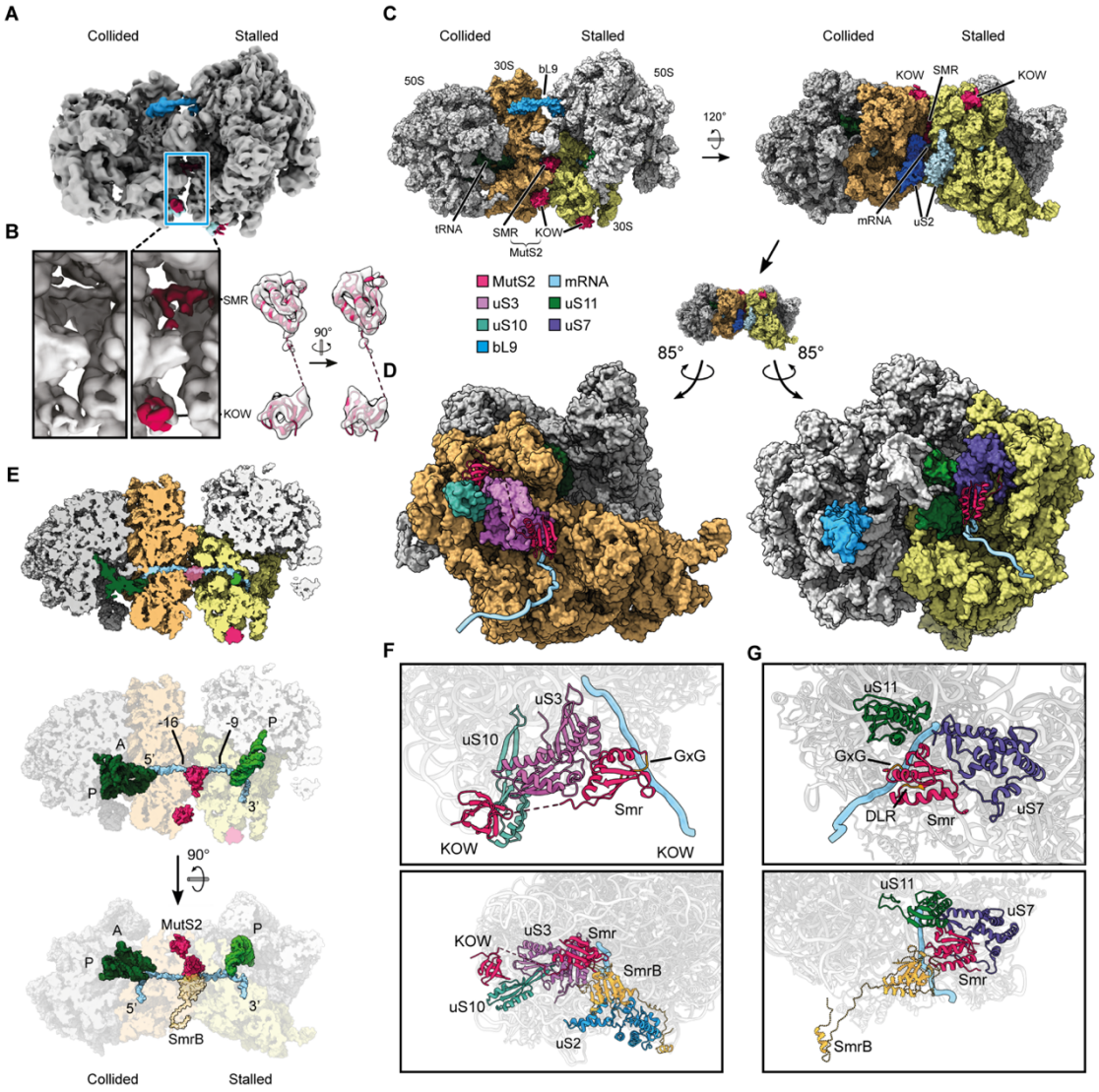
A
Collided
Stalled
B
SMR
KOW
90°
C
Collided
Stalled
50S
30S
bL9
50S
tRNA
SMR
KOW
MutS2
30S
120°
KOW
SMR
KOW
mRNA
uS2
MutS2
mRNA
uS3
uS11
uS10
uS7
bL9
85°
85°
D
E
-16
-9
P
A
5'
P
3'
90°
A
MutS2
P
P
5'
3'
SmrB
Collided
Stalled
F
uS3
uS10
GxG
Smr
KOW
KOW
KOW
uS3
Smr
SmrB
uS10
uS2
G
uS11
GxG
DLR
Smr
uS7
uS11
uS7
Smr
SmrB

Figure 2.5 Cryo-EM structure of the MutS2 KOW and SMR domains binding the *B. subtilis* disome. (A) Experimental cryo-EM reconstruction, lowpass-filtered, with MutS2 in red, uS10 in light blue and bL9 in blue. (B) Left: Zoomed-in view of the inter-ribosomal interface of a class of particles without (left) and with (right) MutS2. Right: Fit of the MutS2 KOW and SMR domains into the experimental density. (C) Cryo-EM structure of the collided B. subtilis disome bound by MutS2 KOW and SMR domains. (D) Interactions of MutS2 with the collided disome interface, seen from each side of that interface. (E) Top, Middle: Cut view of the MutS2-bound disome showing the mRNA path and the position of the KOW and SMR domains as well as tRNA (green) in both ribosomes. Bottom: Comparison of the position of MutS2 in the *B. subtilis* disome to that of SmrB in the E. coli disome. (F) Top: Close-up view of the conformation and interactions of MutS2 on the collided ribosome side of the interface. Bottom: Overlay of the same with the *E. coli* SmrB structure from Saito *et al* (matched to the *B. subtilis* structure by aligning uS2 from both structures). (G) Top: Close-up view of the conformation and interactions of MutS2 on the stalled ribosome side of the interface. Bottom: Overlay of the same with the *E. coli* SmrB structure from Saito *et al*.

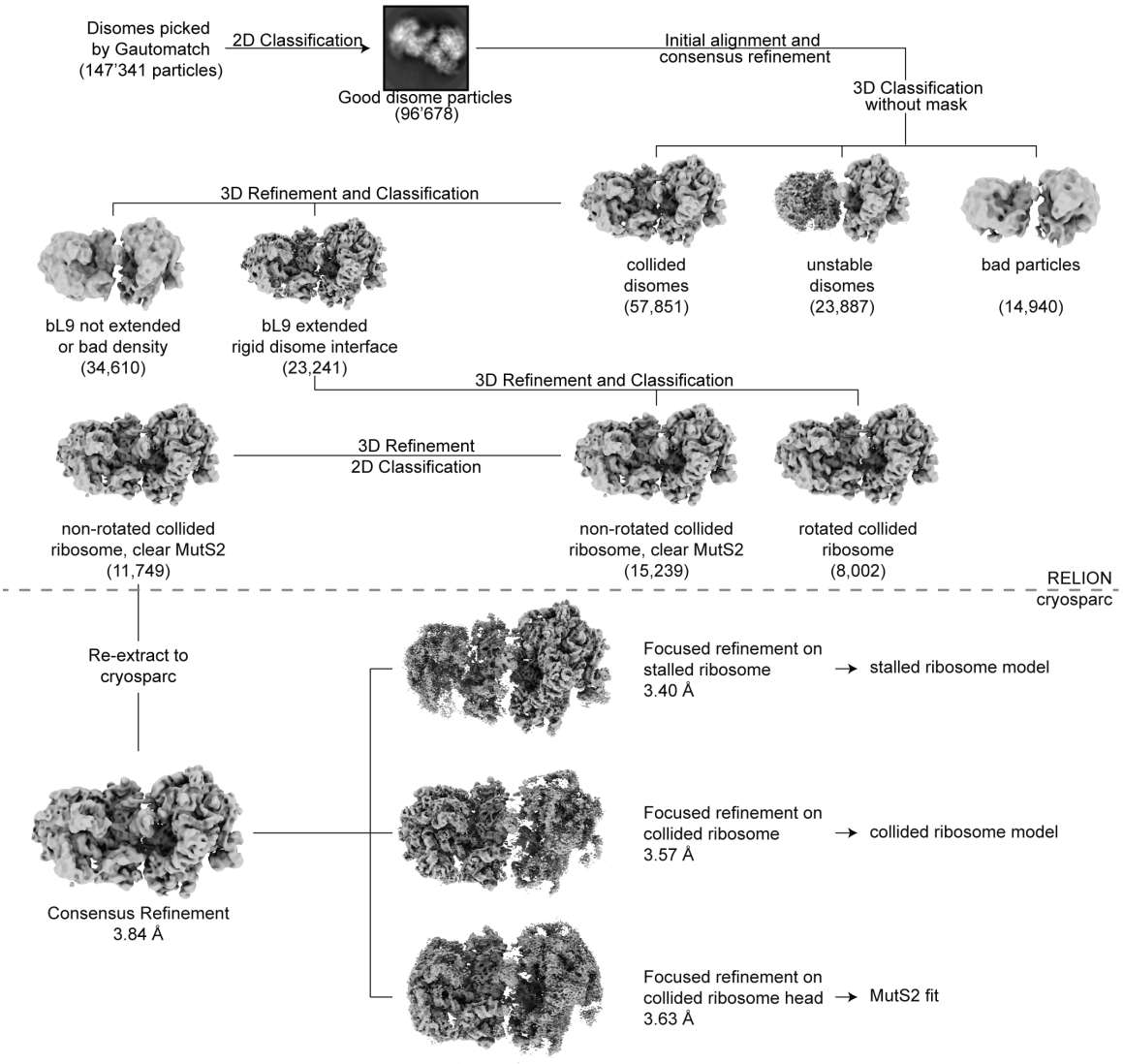
Disomes picked
by Gautomatch
(147'341 particles)
2D Classification
Good disome particles
(96'678)
Initial alignment and
consensus refinement
3D Classification
without mask
collided
disomes
(57,851)
unstable
disomes
(23,887)
bad particles
(14,940)
3D Refinement and Classification
bL9 not extended
or bad density
(34,610)
bL9 extended
rigid disome interface
(23,241)
3D Refinement and Classification
3D Refinement
2D Classification
non-rotated collided
ribosome, clear MutS2
(11,749)
non-rotated collided
ribosome, clear MutS2
(15,239)
rotated collided
ribosome
(8,002)
RELION
cryosparc
Re-extract to
cryosparc
Consensus Refinement
3.84 Å
Focused refinement on
stalled ribosome
3.40 Å
stalled ribosome model
Focused refinement on
collided ribosome
3.57 Å
collided ribosome model
Focused refinement on
collided ribosome head
3.63 Å
MutS2 fit

Figure 2.6 Processing scheme for reconstituted MutS2-disome complex. Shown are the principal steps of processing as well as representative reconstructions for each step. Initial processing steps and classification were performed in Relion, followed by high-resolution refinement of the resulting class of particles in CryoSPARC.

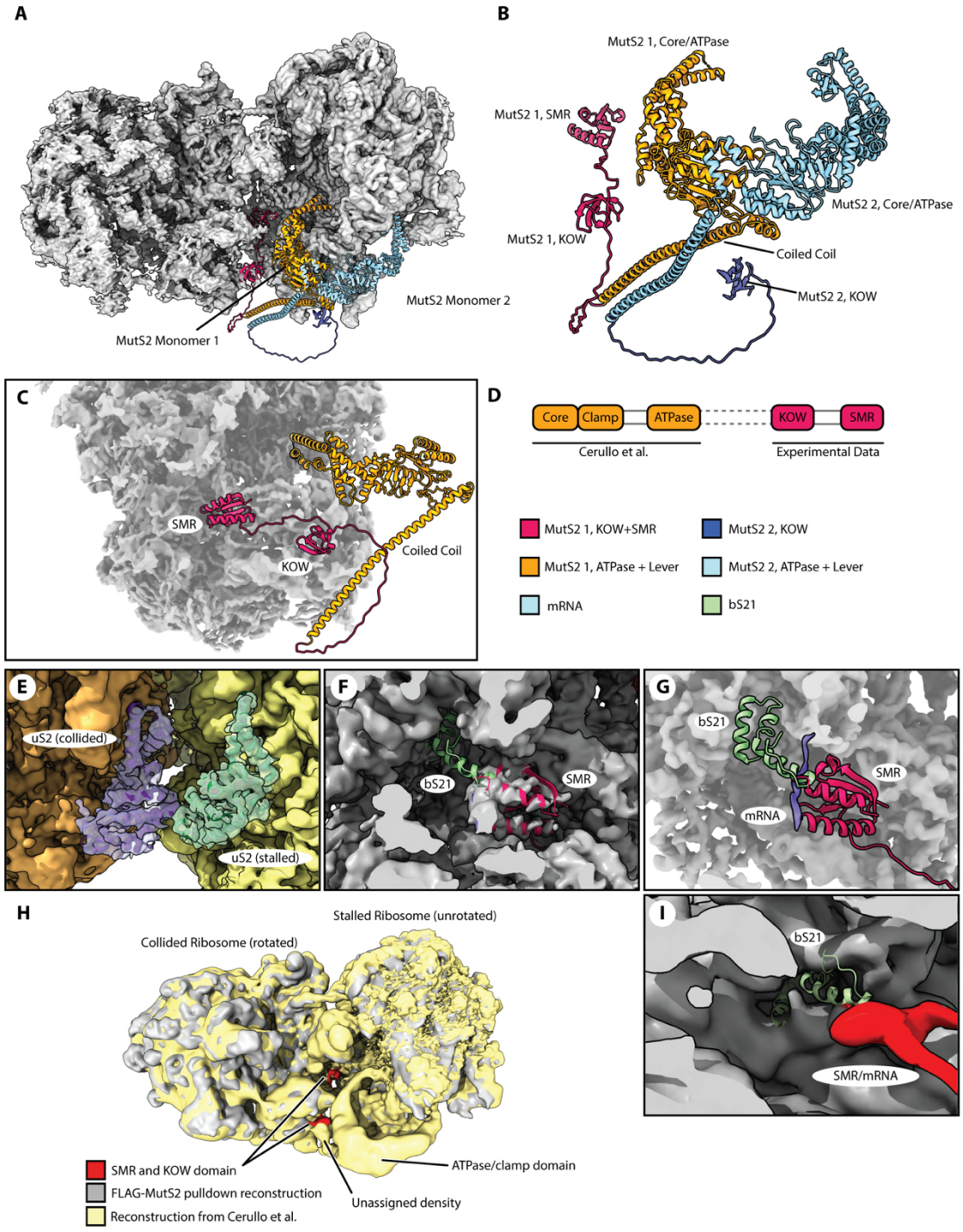
A
MutS2 Monomer 1
MutS2 Monomer 2
B
MutS2 1, Core/ATPase
MutS2 1, SMR
MutS2 2, Core/ATPase
MutS2 1, KOW
Coiled Coil
MutS2 2, KOW
C
SMR
KOW
Coiled Coil
D
Core
Clamp
ATPase
KOW
SMR
Cerullo et al.
Experimental Data
MutS2 1, KOW+SMR
MutS2 2, KOW
MutS2 1, ATPase + Lever
MutS2 2, ATPase + Lever
mRNA
bS21
E
uS2 (collided)
uS2 (stalled)
F
bS21
SMR
G
bS21
SMR
mRNA
H
Stalled Ribosome (unrotated)
Collided Ribosome (rotated)
SMR and KOW domain
FLAG-MutS2 pulldown reconstruction
Reconstruction from Cerullo et al.
ATPase/clamp domain
Unassigned density
I
bS21
SMR/mRNA

Figure 2.7 MutS2 KOW and SMR domains bind the ribosome in a manner congruent with previous studies on the MutS2 Core/ATPase domains. (A) Experimental cryo-EM map (gray) and model of the MutS2 dimer binding a collided disome in *B. subtilis*. The SMR and KOW domains of MutS2 monomer 1 (red) as well as the KOW domain of MutS2 monomer 2 (violet) recruit the MutS2 are visible in the cryo-EM reconstruction. The Core/ATPase domains are not visible in the reconstruction, but the structure as published by Cerullo *et al* (monomer 1: yellow, monomer 2: light blue) is congruent with our experimental observations. (B) Isolated view of the composite structure of the MutS2 dimer: The length of the flexible loop between coiled-coil and KOW domains does not allow a stringent assignment of either KOW domain to either monomer from the Cerullo *et al* structure, hence the assignment shown here was chosen arbitrarily. (C) Side view of MutS2 monomer 1 engaged with the stalled ribosome. (D) Schematic representation of the composite structure of MutS2 shown in (A, B). (E) Map-to-model fit of uS2 from both stalled and collided ribosome to a composite map of the MutS2-bound *B. subtilis* disome. (Stalled and collided ribosome maps were refined separately). uS2 is clearly present on both ribosomes in the complex. (F) Fit of the MutS2 monomer 1 SMR domain into the experimental density and comparison with the hypothetical location of bS21 as observed by Cerullo *et al*. In our experimental data, there is no evidence that bS21 is present in the MutS2-bound collided disomes. (G) Representation of the experimentally determined location of the MutS2 monomer 1 SMR domain and the position of bS21 as observed in Cerullo *et al*. bS21 would clash with the observed conformation of MutS2 SMR next to the mRNA. (H) Overlay of the experimental cryo-EM map of the MutS2-bound disome published by Cerullo *et al* and the experimental map of disomes collected from a FLAG-MutS2 pulldown in our experiments. SMR and KOW domain are highlighted in our experimental map. Both ribosomes match in their rotation states, the stalled ribosome being non-rotated in both maps and the collided ribosome rotated. MutS2 ATPase/Core/Clamp domains are visible only in the reconstruction from Cerullo *et al*, while the SMR domain is visible in our reconstruction. An extra density in the map of Cerullo *et al* that was not assigned in the original publication is visible close to the position of the KOW domain identified in our data. (I) Close-up view of the binding pocket for bS21 in our *in vivo* dataset. Only very weak partial density can be observed for bS21 compared to surrounding ribosomal proteins and the density corresponding to mRNA and the MutS2 SMR domain.

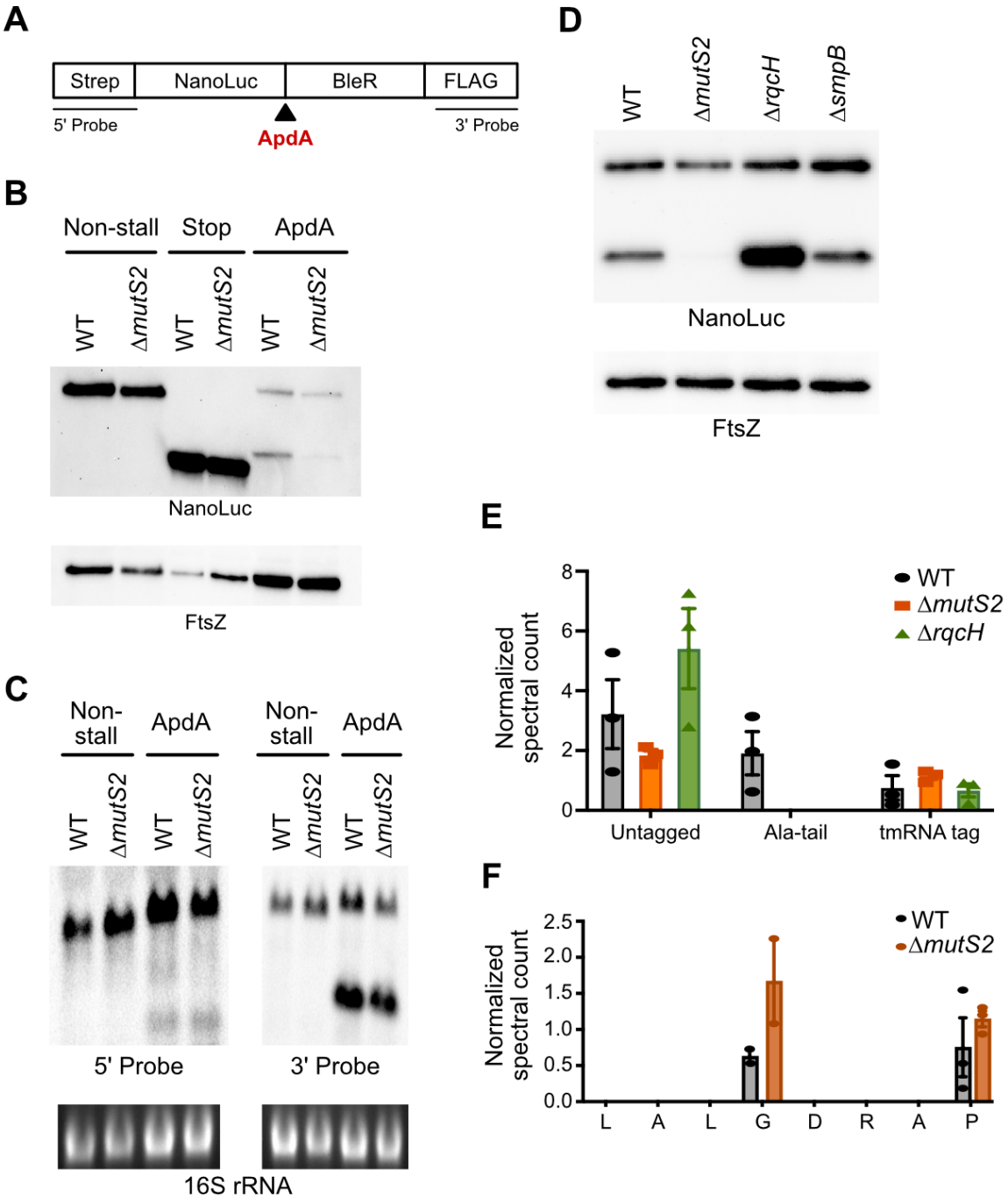
A
Strep
NanoLuc
BleR
FLAG
5' Probe
ApdA
3' Probe
B
Non-stall
Stop
ApdA
WT
ΔmutS2
NanoLuc
FtsZ
C
Non-stall
ApdA
5' Probe
3' Probe
16S rRNA
D
WT
ΔmutS2
ΔrqcH
ΔsmpB
NanoLuc
FtsZ
E
Normalized spectral count
WT
ΔmutS2
ΔrqcH
Untagged
Ala-tail
tmRNA tag
F
Normalized spectral count
WT
ΔmutS2
L A L G D R A P

Figure 2.8 MutS2 rescues ribosomes stalled in the middle of an ORF. (A) Schematic of stalling reporter for studying ribosome rescue in *B. subtilis*. Between the NanoLuc gene and bleomycin resistance gene, we inserted either no additional sequence (Non-stall), stop codons (Stop), or the ApdA stalling motif. (B) Reporter protein from wild-type and *ΔmutS2* strains was detected by anti-NanoLuc antibodies. The FtsZ protein serves as a loading control. (C) Northern blots of reporter mRNA using the 5'-probe and the 3'-probe. Ethidium bromide staining of the 16 S rRNA serves as a loading control. (D) Reporter protein from wild-type, ΔmutS2, ΔrqcH, and ΔsmpB strains was detected by anti-NanoLuc antibodies. The FtsZ protein serves as a loading control. (E) The addition of the tmRNA tag or the Ala-tail at the stall site of the reporter in wild-type, *ΔmutS2*, and *ΔrqcH* strains was detected by LC-MS/MS. The spectral counts are normalized to a different peptide from the reporter protein. The mean of three biological replicates and the standard error are shown. (F) tmRNA tagging levels along the stalling sequence in wild-type and *ΔmutS2* strains are not dependent on MutS2. The mean of three biological replicates and the standard error are shown.

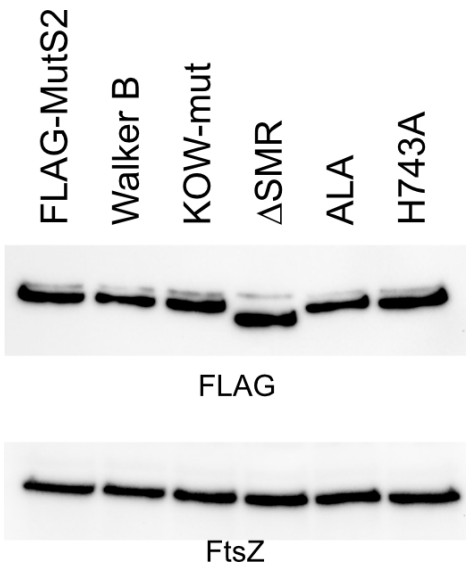
FLAG-MutS2
Walker B
KOW-mut
ΔSMR
ALA
H743A
FLAG
FtsZ

Figure 2.9 Expression levels of MutS2 mutants are similar. Levels of FLAG-tagged constructs of MutS2 in *B. subtilis* cells were detected on a western blot using an anti-FLAG antibody. The FtsZ protein serves as a loading control.

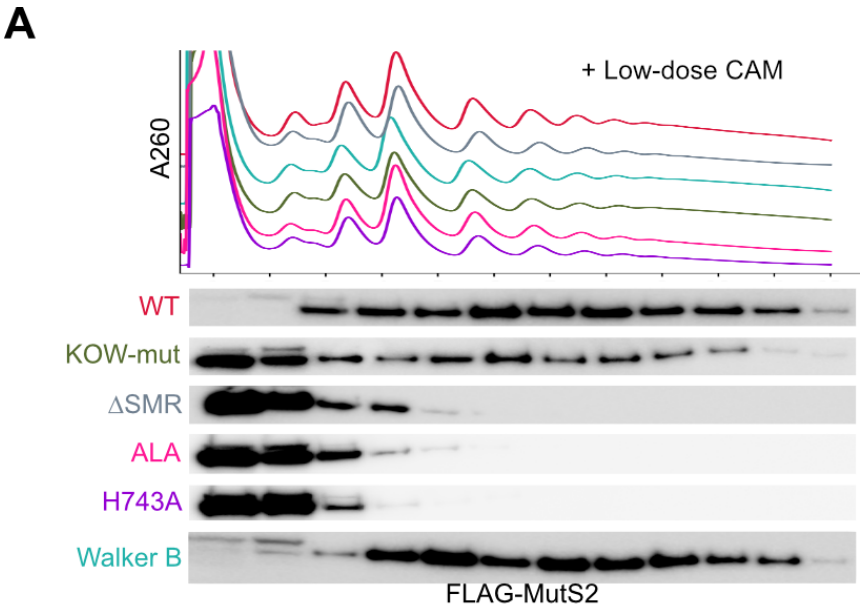
A
+ Low-dose CAM
A260
WT
KOW-mut
ΔSMR
ALA
H743A
Walker B
FLAG-MutS2

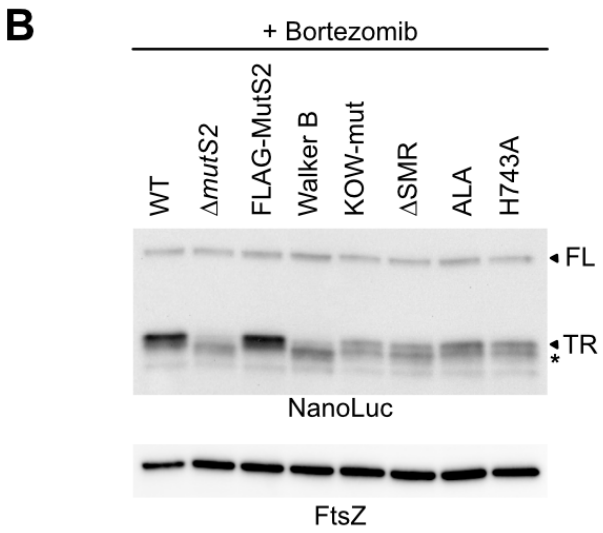
B
+ Bortezomib
WT
ΔmutS2
FLAG-MutS2
Walker B
KOW-mut
ΔSMR
ALA
H743A
FL
TR
*
NanoLuc
FtsZ

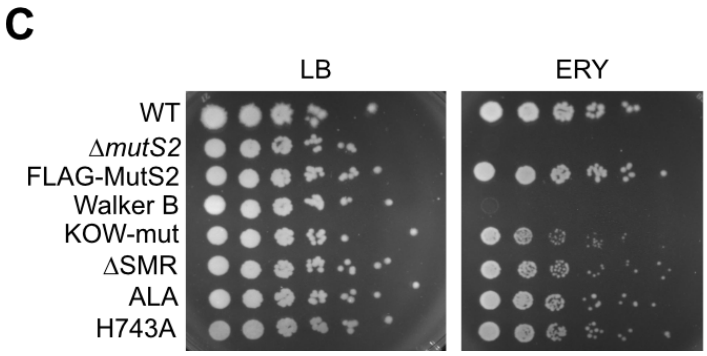
C
LB
ERY
WT
ΔmutS2
FLAG-MutS2
Walker B
KOW-mut
ΔSMR
ALA
H743A

Figure 2.10 Activities of the SMR and ATPase domains of MutS2. (A) Following induction of ribosome collisions with CAM, the distribution of Flag-tagged MutS2 and several mutants was determined by fractionation over sucrose gradients and detection with anti-FLAG antibody. ΔSMR is missing the SMR domain (residues 710–785). The Walker B mutant prevents ATP hydrolysis (E416A). KOW-mut contains mutations to the KOW domain to perturb binding to uS10 (Q668xxILK to A668xxAAA). ALA and H743A are mutations to conserved residues in the SMR domain. (B) Cells expressing various constructs of MutS2 were grown with 20 μM bortezomib to inhibit ClpXP activity and reporter protein was visualized using an anti-NanoLuc antibody. FL = full-length ApdA reporter protein, TR = truncated reporter protein, * = smaller truncated protein not dependent on MutS2 activity. The FtsZ protein serves as a loading control. (C) Spotting assay of strains expressing various MutS2 constructs on plates with and without erythromycin (0.08 μg/mL).

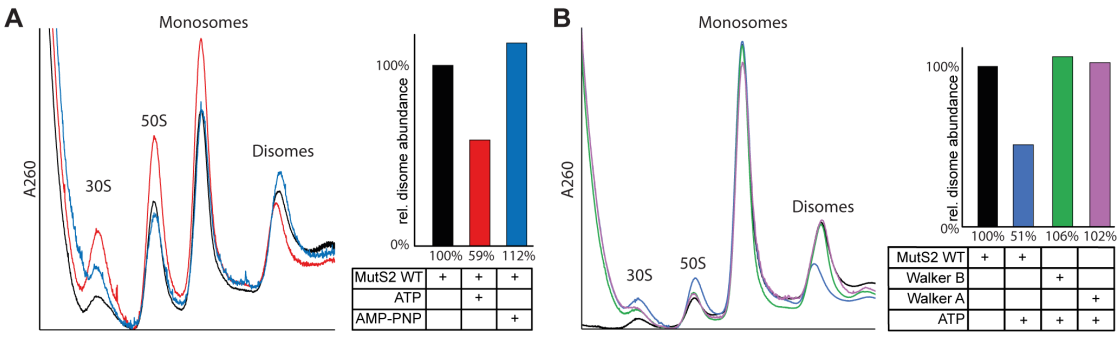
A
Monosomes
50S
30S
Disomes
A260
100%
0%
rel. disome abundance
100% 59% 112%
MutS2 WT + + +
ATP + +
AMP-PNP +
B
Monosomes
30S
50S
Disomes
A260
100%
0%
rel. disome abundance
100% 51% 106% 102%
MutS2 WT + + +
Walker B + +
Walker A +
ATP + + +

Figure 2.11 MutS2 splits stalled ribosomes into subunits *in vitro*. (A) Left: UV chromatograms from sucrose gradient fractionation of disome splitting assays with MutS2 WT. Right: Relative abundance of disomes compared to total ribosomal fractions after splitting reaction in experiments with MutS2 WT, calculated from relative peak areas in the chromatograms by dividing the disome peak area by the total peak area of subunits, monosomes, and disomes. Purified *B. subtilis* disomes were used as input. Only in the presence of ATP do we observe a significant decrease in the abundance of disomes compared to other ribosomal fractions after incubation with MutS2. (B) Left: UV chromatograms from sucrose gradient fractionation of disome splitting assays with MutS2 WT and ATPase ("Walker B": E416A, "Walker A": G340R) mutants. Right: Relative abundance of disomes computed as above. Purified *B. subtilis* disomes were used as input. Mutations that render either the Walker A or Walker B motifs non-functional abrogate the disome splitting activity of MutS2 entirely.

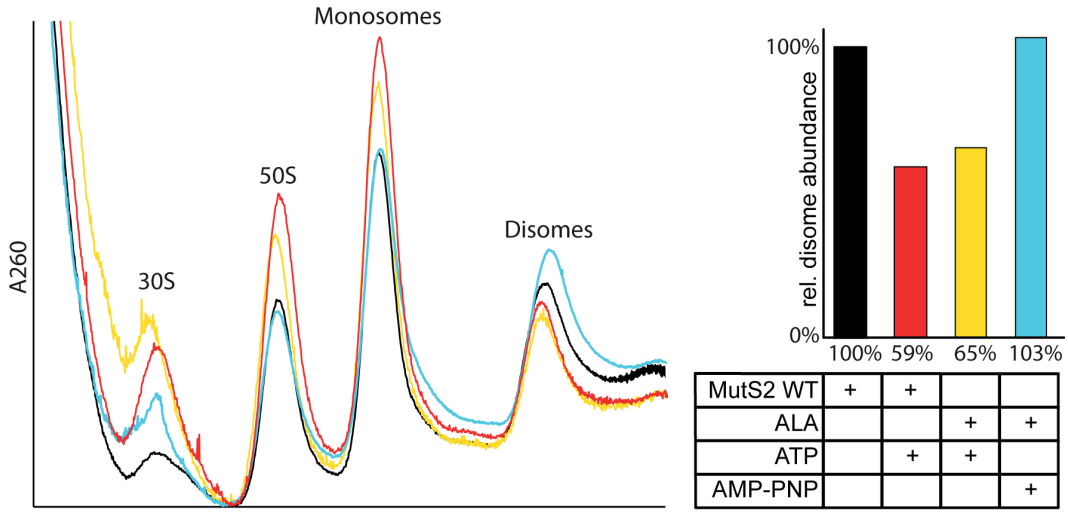
Monosomes
50S
Disomes
30S
A260
100%
rel. disome abundance
0%
100% 59% 65% 103%
MutS2 WT + +
ALA + +
ATP + +
AMP-PNP +

Figure 2.12 The DLR motif of MutS2 SMR domain is not essential for disome splitting. Left: UV chromatograms from sucrose gradient fractionation of disome splitting assays with MutS2 WT and MutS2 D711LR to A711LA mutant ("ALA"). Right: Relative abundance of disomes compared to total ribosomal fractions after splitting reaction, calculated from relative peak areas in the chromatograms. Purified *B. subtilis* disomes were used as input. The presence of the mutation has no effect on the efficiency of the splitting reaction either with or without hydrolysable ATP, indicating that the DLR motif of the SMR domain is not required for this process.

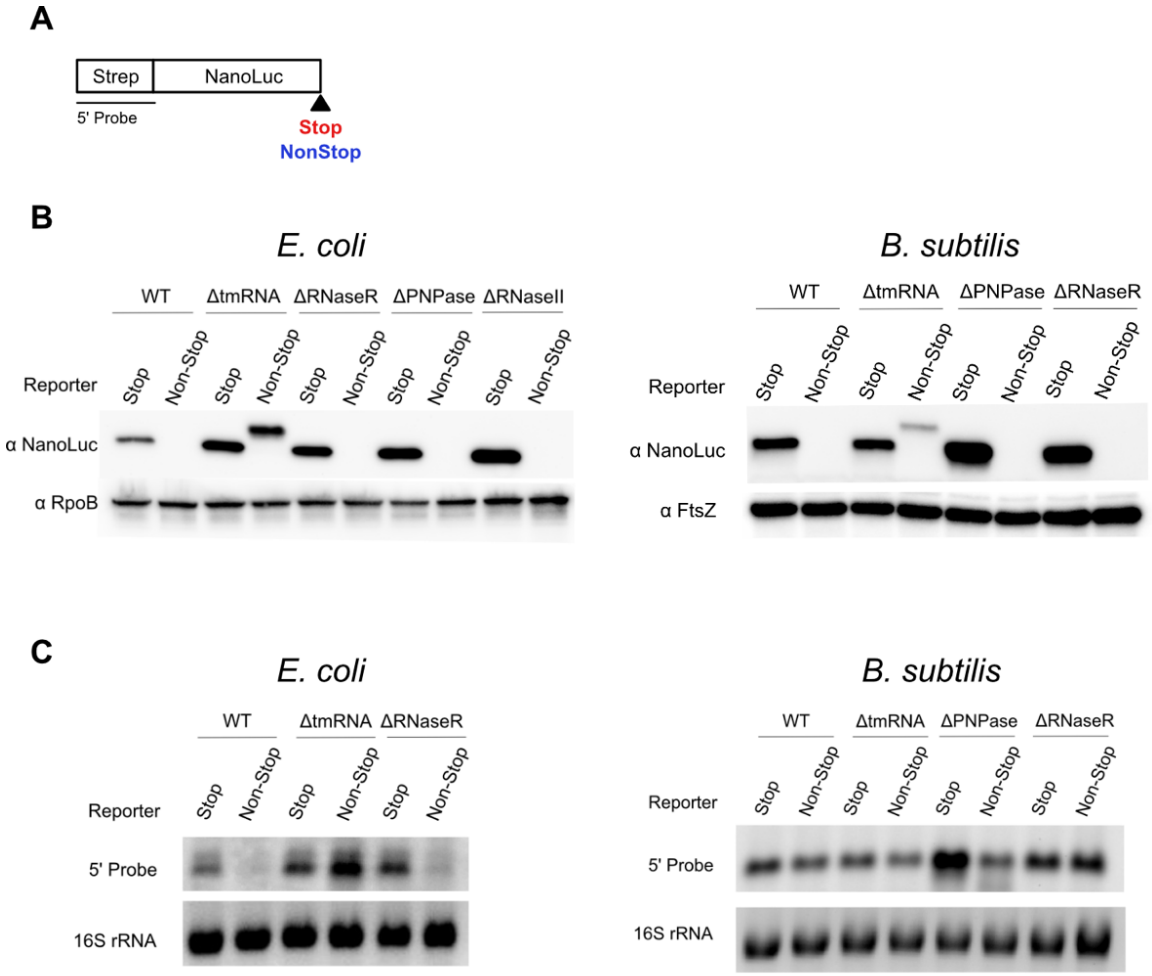
A
Strep
NanoLuc
5' Probe
Stop
NonStop
B
E. coli
WT
ΔtmRNA
ΔRNaseR
ΔPNPase
ΔRNaseII
Reporter
Stop
Non-Stop
α NanoLuc
α RpoB
B. subtilis
WT
ΔtmRNA
ΔPNPase
ΔRNaseR
Reporter
α NanoLuc
α FtsZ
C
E. coli
WT
ΔtmRNA
ΔRNaseR
Reporter
5' Probe
16S rRNA
B. subtilis
WT
ΔtmRNA
ΔPNPase
ΔRNaseR
Reporter
5' Probe
16S rRNA

Figure 2.13 Comparison of NonStop reporter protein and mRNA levels in *E. coli* and *B. subtilis*. (A) Schematic of Stop and NonStop reporters. (B) Western blots showing levels of reporter protein levels in *E. coli* and *B. subtilis*. For both strains, the Nonstop reporter is detected only in tmRNAΔ. Reporter protein was detected by using an anti-NanoLuc antibody. The anti-FtsZ and anti-RpoB was used for loading controls. (C) Northern blots showing reporter mRNA levels with probes hybridizing to the 5' end of the mRNA. In *E. coli*, the NonStop mRNA is stable only when tmRNA is deleted. In *B. subtilis*, the NonStop reporter is equally stably in all strains. 16S rRNA stained by ethidium bromide is shown as the loading control.

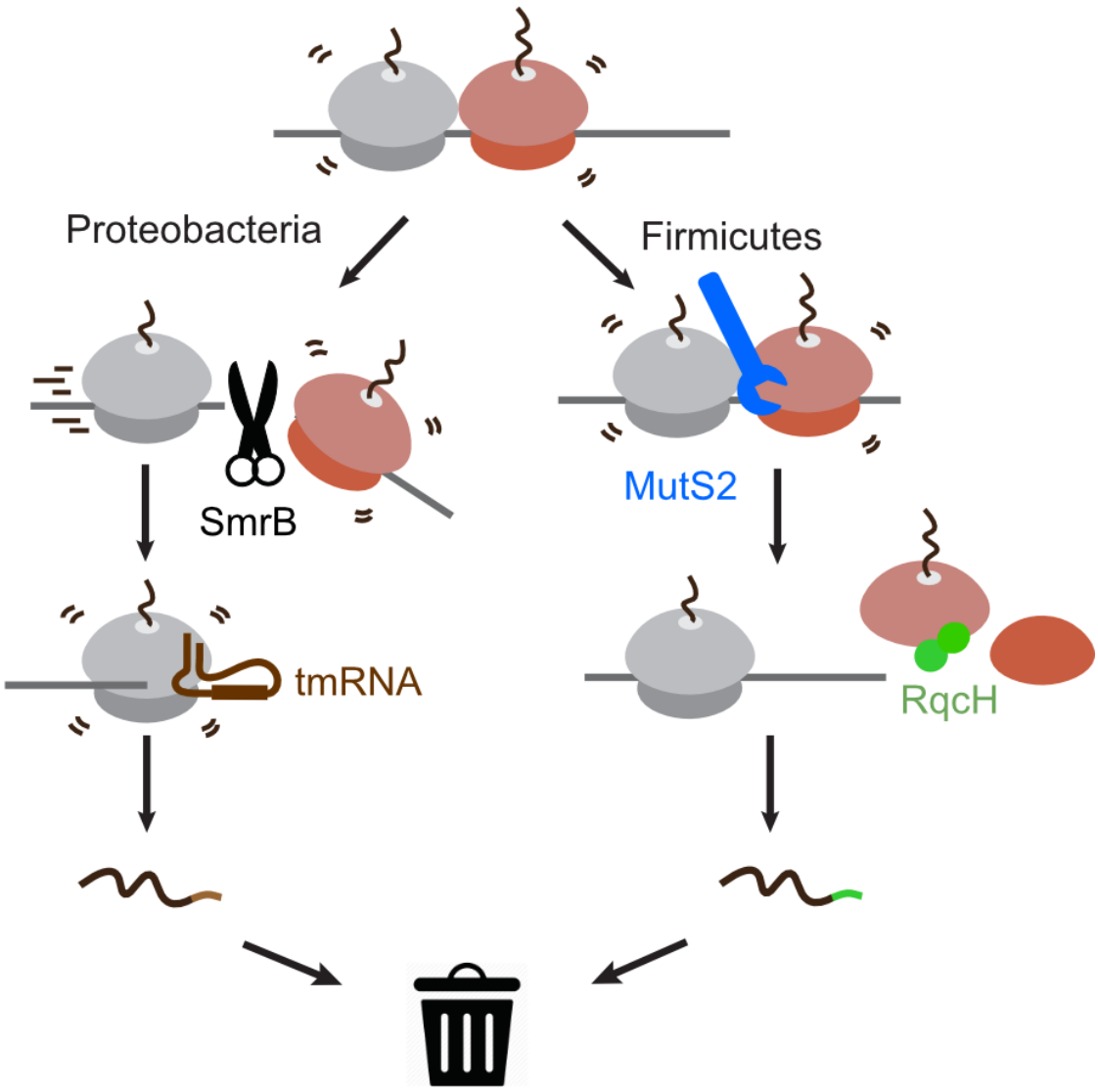
Proteobacteria
Firmicutes
SmrB
MutS2
tmRNA
RqcH

Figure 2.14 Model for ribosome rescue in bacteria. Proteobacteria containing SmrB rescue collided ribosomes via nucleolytic cleavage while firmicutes and other bacteria containing MutS2 split collided ribosomes into subunits. These differences mean that different pathways (tmRNA or RqcH) tag the nascent polypeptide to target it for degradation by proteases.

Chapter 3: Conclusion

The work shown in this thesis reveals the mechanism of ribosome rescue in *B. subtilis*. Previous work from our lab showed that in *E. coli*, the endonuclease, SmrB, recognizes collided ribosomes and cleaves the mRNA in between them using its SMR domain[52]. The work presented in this thesis shows that although *B. subtilis* also contains an SMR domain protein that recognizes collided ribosomes, the mechanism of rescue does not involve mRNA cleavage. SMR domain proteins in bacteria mostly have domain architecture similar to *B. subtilis* MutS2, whereas only proteobacteria have the SmrB domain architecture. This observation solidified the significance of investigating the function of MutS2 as its mechanism of action is more broadly conserved in many phyla of bacteria. SMR proteins are broadly found in bacteria and eukaryotes, and our results suggest that in many cases the SMR domain's role in recognizing ribosome collisions is conserved even when its catalytic activity may not be.

One of the earliest striking differences that we observed between *E. coli* SmrB and *B. subtilis* MutS2 was the phenotypes of the deletion strains. In *E. coli* when SmrB is deleted, the only phenotype found was that cells were hypersensitive to a very high dose of erythromycin[52]. *E. coli* cells lacking SmrB were not hypersensitive to various other elongation inhibitors, RNA damaging agents, and environmental stresses. In contrast, when MutS2 is deleted, *B. subtilis* cells are hypersensitive to a host of elongation inhibitors (erythromycin, chloramphenicol, spectinomycin, etc.) at concentrations similar to the minimum inhibitory concentration (MIC). This suggests

SmrB is not as essential to ribosome rescue as MutS2 is in *B. subtilis*. Could there be an unknown compensatory ribosome rescue pathway in *E. coli* masking the SmrB knockout phenotype? One possibility is that there could be a ribosome splitter in *E. coli* that is the dominant ribosome rescue factor.

Another reason why a ribosome splitter in *E. coli* may be necessary is to rescue ribosomes that are unable to undergo elongation. In *E. coli*, cleavage by SmrB creates a nonstop message which is the canonical target for the trans-translation rescue pathway[52]. Trans-translation requires that the stalled ribosome be able to resume translation on the ORF of tmRNA. However, when ribosomes are bound by elongation inhibitors, they are unable to perform normal elongation. In these instances, rescuing ribosomes by splitting would be more effective than relying on tmRNA. Therefore, another rescue factor in addition to SmrB might be required to rescue different stalled ribosome substrates. Further experiments would be necessary to identify such a factor.

Not only are ribosome collisions rescued differently in *B. subtilis*, the mechanism of tagging the nascent peptide is also drastically different than *E. coli*. In *E. coli*, the nascent peptide is tagged with the tmRNA degron tag encoded as the stalled ribosome resumes translation on the ORF of tmRNA. In *B. subtilis*, after MutS2 splits the stalled ribosomes into subunits, the large subunit still contains a nascent chain and a peptidyl-tRNA. The nascent chain receives a degron tag which is a poly-alanine sequence that is added through a non-templated addition to the nascent peptide. This process is facilitated by the factor RqcH, a homolog of Rqc2 found in yeast. RqcH brings tRNAs aminoacylated with alanine to the post-split 50S subunit in a process called Ala-

tailing[57,59–61]. This alanine tail marks the nascent chain for degradation by ClpXP. RqcH homologs are found in eukaryotes, bacteria, and archaea indicating that they may have been present in the last universal common ancestor (LUCA)[57]. However, many bacterial phyla have lost RqcH homologs such as *E. coli*. Interestingly, RqcH and MutS2 strongly co-occur further supporting their functional connection[63].

This raises the question how are nascent chains targeted for degradation in *E. coli* when ribosomes are unable to translocate normally. When *E. coli* cells are treated with elongation inhibitors, is there a degron added to the nascent chain when the tmRNA ORF cannot be translated? Although *E. coli* does not possess a RqcH homolog they do possess a homolog to RqcP. RqcP also binds to a 50S subunit with a nascent chain and peptidyl-tRNA still attached. RqcP positions the Ala-tRNA, recruited by RqcH, so that Ala-tailing can occur. Previous work by others have shown that RqcP is essential to Ala-tailing[59–61]. The *E. coli* homolog of RqcP is called Hsp15, and recent cryo-EM structures show that it binds to large subunits with a nascent chain and peptidyl-tRNA still attached[99]. In fact, when comparing RqcP binding and Hsp15 binding, they bind to analogous positions on the 50S. Although the exact role of Hsp15 in *E. coli* is yet to be fully determined, a similar function in RQC is the running hypothesis.

Another question that arises from our work is if there are endogenous substrates of MutS2. The current work utilizes antibiotic treatment to induce collisions globally or a stalling reporter to be a substrate for MutS2. Maybe there are endogenous substrates whose translation is regulated by MutS2. One way to identify these substrates would be through ribosome profiling. Comparing ribosome profiling data from wild-type *B. subtilis*

and the MutS2 knockout strain may reveal endogenous substrates. If translation of a transcript is dependent on MutS2, then there would be a pile up of ribosome footprint densities on that transcript in a MutS2 deletion strain as compared to wild-type *B. subtilis*. In yeast, this strategy was used to identify an example of endogenous RQC substrate, the gene SDD1, which contains a polybasic stretch that causes ribosome stalling. Ribosome profiling data showed that ribosome footprints upstream of the stall site accumulated in Hel2 deletion strains as compared to wild-type *S. cerevisiae*[44].

Other experiments in *S. cerevisiae* found that RQC is essential under various stress conditions. Alkylative and oxidative stresses damage mRNAs in cells and cause ribosomes to stall. Ribosomes stalled on damaged mRNAs are rescued by the RQC pathway highlighting the importance of this pathway in maintaining cellular homeostasis[100]. In fact, recent work by our lab and others shows that in mammalian cells, ribosome collisions occur due to various stresses (nutrient starvation, UV, etc.), and the cell surmounts a general stress response depending on the severity of the ribotoxic stress[101,102]. The trans-translation pathway has long been shown to be important for bacteria in conditions of stress such as carbon starvation, heat, etc.[10,103] This further highlights the importance of ribosome rescue pathways in dealing with environmental stresses. Therefore, the RQC pathways may also be necessary for bacteria to survive or recover from various environmental stresses.

On top of the mechanistic differences in rescuing collided ribosomes between *E. coli* and *B. subtilis*, there seems to be an underlying difference in the way that problematic mRNAs are dealt with in the two bacterial species. Whether it is stalling in

the middle of an ORF or stalling at the end of transcripts, in *B. subtilis* rescue of stalled ribosomes is not linked to preferential decay of the mRNAs like it is in *E. coli*.

The observed differences in mRNA dynamics could be due to several reasons, such as different levels of transcription-translation coupling. In some bacteria, transcription and translation can occur simultaneously at least in some genes. As nascent mRNAs exit out of RNA polymerase, ribosomes initiate translation when the ribosome binding site becomes accessible. In *E. coli* the speeds of polymerase and the ribosome are similar because they are coupled. Transcription-translation coupling is also important for gene regulation. A prime example is the *trp* operon. The *trp* operon is regulated by attenuation in *E. coli*; when tryptophan (Trp) levels are high, the ribosome translates without pausing, allowing the nascent mRNA to form a hairpin and terminate transcription before transcribing the full operon. However, when Trp levels are low, the ribosome pauses at Trp codons early in the operon. This pause allows an anti-terminator structure to form behind the polymerase so that transcription continues for the full *trp* operon encoding tryptophan biosynthesis enzymes. Thus, the levels of tryptophan in the cell directly control the synthesis of tryptophan[104].

In addition, most *E. coli* transcripts utilize Rho-dependent transcription termination. Rho is ring-shaped hexameric ATPase that acts as a molecular motor and applies a mechanical force onto the elongating polymerase to terminate transcription. Rho recognizes a long C-rich RNA sequence called the Rho utilization (rut) site to load and close its ring on the nascent RNA[105]. Therefore, a ribosome translating closely behind the polymerase is required to prevent premature Rho binding and termination.

Only when the ribosome terminates translation and is removed can Rho bind to the rut sites on the mRNA and terminate transcription.

Another line of evidence for transcription-translation coupling in *E. coli* comes from structural biology. In recent years, cryo-EM structures of RNA polymerase and the ribosome (deemed the "expressome") have been solved in various states. One structure showed that the ribosome and polymerase are bridged by transcription factors NusA and NusG[106]. In fact, *in vitro* experiments showed that NusG is essential for coupling and prevents RNA polymerase from back tracking[107]. Recent structures and single molecule work have further corroborated the functional role of the expressome showing that a coupled ribosome helps transcription stay processive by mechanical and allosteric influences[108].

Unexpectedly, however, in *B. subtilis*, transcription and translation are mostly uncoupled. The rate of transcription is twice as fast as the rate of translation. Most transcripts also utilize Rho-independent transcription termination which does not utilize factors to mediate termination and rather uses structure formations such as hairpins. Thus, ribosomes do not need to closely follow RNA polymerase[109]. This leads to different regulatory strategies in *B. subtilis* compared to *E. coli*. In *B. subtilis*, tryptophan biosynthesis is also regulated by tryptophan levels, but rather than using a ribosome pausing mechanism, *B. subtilis* contain a complex called the tryptophan-activated RNA-binding attenuation protein (TRAP). TRAP is activated in conditions with excess tryptophan and binds to the nascent transcript of the *trp* operon preventing anti-terminator formation and promoting terminator formation. This inhibits tryptophan

biosynthesis[110]. This clearly shows how *B. subtilis* and *E. coli* achieve the same goal of sensing tryptophan levels in the cell to tune biosynthesis of tryptophan but through different mechanisms. More generally, *B. subtilis* have reduced transcriptional attenuation as compared to *E. coli* and instead often utilize transcription-controlling riboswitches[111].

Work from Gene-wei Li's group predicted the presence of transcription-translation coupling in all phyla of bacteria using a metric based on distances between stop codons and transcription terminators. In bacteria such as *B. subtilis*, because transcription is twice as fast as translation and uncoupled from translation, the distances between the stop codon and the terminator are predominantly short; 72% of genes have a distance of 12 nucleotides or shorter[109]. In contrast, terminators have to be farther downstream in *E. coli* so that the ribosome does not interfere with hairpin formation. When we compared SMR domains between phyla of bacteria with predicted coupling of transcription and translation, we noticed that most bacteria with predicted transcription-translation coupling contain SmrB while uncoupled bacteria have a MutS2-like SMR protein. Although this correlation does not definitively suggest a connection, this difference in coupling between *E. coli* and *B. subtilis* may be a reason for the need for different ribosome rescue mechanisms. For example, in *E. coli*, ribosome collisions may occur right near RNA polymerase. Therefore, cleaving the mRNA in between by SmrB may also be beneficial, clearing the congestion. On the other hand, because transcription and translation are mostly uncoupled in *B. subtilis*, there may not have been a need for mRNA cleavage, and splitting may be sufficient to relieve the stress

ribosome stalling is causing to the cell. Experiments inducing RNA polymerase pausing in *E. coli* and *B. subtilis* and monitoring the mRNA and protein output could be one way to investigate this hypothesis.

Another major difference between *E. coli* and *B. subtilis* is the differing mRNA decay mechanisms. In *E. coli*, mRNAs are decayed in the 3' to 5' direction by exonucleases. However, in *B. subtilis*, mRNA decay mainly occurs in the 5' to 3' direction[95]. The presence of the 5' to 3' exonuclease in *B. subtilis* may be the reason why ribosome rescue is not coupled to mRNA decay in *B. subtilis* because the ribosome binding site would be rapidly decayed preventing further ribosome loading. However, in *E. coli* ribosomes could continue to load on problematic mRNAs, and so rapidly decaying the problematic mRNAs would be beneficial for the cell. One difficulty with designing experiments to test this hypothesis is that the 5' to 3' exonuclease in *B. subtills*, RNase J, is encoded by an essential gene. Also, many 3' to 5' exonucleases in *E. coli* and *B. subtilis* are known to be compensatory, so knocking one of them out may not be enough to see effects[95]. A bioinformatic approach could be used to analyze the presence of either SmrB and MutS2 and various mRNA decay machinery components to deduce any correlations. The ability of an SMR domain to cleave the mRNA may be correlated with the presence of certain exo- and/or endonucleases.

The overall thesis work clearly shows the divergent mechanisms of ribosome rescue employed by *E. coli* and *B. subtilis*. Additional questions and experiments proposed here would further address the reasons for the diversity and the functional implications to the cell. The surprising finding of the lack of an mRNA decay connection

to ribosome rescue in *B. subtilis* further contributes to the field of ribosome rescue in bacteria which historically mostly studied the events in *E. coli*.

Bibliography

1. Hunt, J. F. *et al.* Nucleotide control of interdomain interactions in the conformational reaction cycle of SecA. *Science* **297**, 2018–2026 (2002).
2. Murakami, A., Nakatogawa, H. & Ito, K. Translation arrest of SecM is essential for the basal and regulated expression of SecA. *Proc. Natl. Acad. Sci. U. S. A.* **101**, 12330–12335 (2004).
3. Woolstenhulme, C. J. *et al.* Nascent peptides that block protein synthesis in bacteria. *Proc. Natl. Acad. Sci. U. S. A.* **110**, E878-887 (2013).
4. Nakatogawa, H. & Ito, K. Intraribosomal regulation of expression and fate of proteins. *Chembiochem Eur. J. Chem. Biol.* **5**, 48–51 (2004).
5. Sakiyama, K., Shimokawa-Chiba, N., Fujiwara, K. & Chiba, S. Search for translation arrest peptides encoded upstream of genes for components of protein localization pathways. *Nucleic Acids Res.* **49**, 1550–1566 (2021).
6. Moss, M. J., Chamness, L. M. & Clark, P. L. The Effects of Codon Usage on Protein Structure and Folding. *Annu. Rev. Biophys.* (2023) doi:10.1146/annurev-biophys-030722-020555.
7. Zhou, M. *et al.* Non-optimal codon usage affects expression, structure and function of clock protein FRQ. *Nature* **495**, 111–115 (2013).
8. Zhou, M., Wang, T., Fu, J., Xiao, G. & Liu, Y. Nonoptimal codon usage influences protein structure in intrinsically disordered regions. *Mol. Microbiol.* **97**, 974–987 (2015).

9. Yan, L. L. & Zaher, H. S. How do cells cope with RNA damage and its consequences? *J. Biol. Chem.* **294**, 15158–15171 (2019).
10. Thomas, E. N., Kim, K. Q., McHugh, E. P., Marcinkiewicz, T. & Zaher, H. S. Alkylative damage of mRNA leads to ribosome stalling and rescue by trans translation in bacteria. *eLife* **9**, e61984 (2020).
11. Wilson, D. N. Ribosome-targeting antibiotics and mechanisms of bacterial resistance. *Nat. Rev. Microbiol.* **12**, 35–48 (2014).
12. Herzel, L., Stanley, J. A., Yao, C.-C. & Li, G.-W. Ubiquitous mRNA decay fragments in E. coli redefine the functional transcriptome. *Nucleic Acids Res.* **50**, 5029–5046 (2022).
13. Kuo, H. K., Krasich, R., Bhagwat, A. S. & Kreuzer, K. N. Importance of the tmRNA system for cell survival when transcription is blocked by DNA-protein cross-links. *Mol. Microbiol.* **78**, 686–700 (2010).
14. Keiler, K. C., Waller, P. R. H. & Sauer, R. T. Role of a Peptide Tagging System in Degradation of Proteins Synthesized from Damaged Messenger RNA. *Science* **271**, 990–993 (1996).
15. Gottesman, S., Roche, E., Zhou, Y. & Sauer, R. T. The ClpXP and ClpAP proteases degrade proteins with carboxy-terminal peptide tails added by the SsrA-tagging system. *Genes Dev.* **12**, 1338–1347 (1998).
16. Flynn, J. M. *et al.* Overlapping recognition determinants within the ssrA degradation tag allow modulation of proteolysis. *Proc. Natl. Acad. Sci. U. S. A.* **98**, 10584–10589 (2001).

17. Neubauer, C., Gillet, R., Kelley, A. C. & Ramakrishnan, V. Decoding in the absence of a codon by tmRNA and SmpB in the ribosome. *Science* **335**, 1366–1369 (2012).
18. Sundermeier, T. R., Dulebohn, D. P., Cho, H. J. & Karzai, A. W. A previously uncharacterized role for small protein B (SmpB) in transfer messenger RNA-mediated trans-translation. *Proc. Natl. Acad. Sci. U. S. A.* **102**, 2316–2321 (2005).
19. Ivanova, N., Pavlov, M. Y., Felden, B. & Ehrenberg, M. Ribosome Rescue by tmRNA Requires Truncated mRNAs. *J. Mol. Biol.* **338**, 33–41 (2004).
20. Richards, J., Mehta, P. & Karzai, A. W. RNase R degrades non-stop mRNAs selectively in an SmpB-tmRNA-dependent manner. *Mol. Microbiol.* **62**, 1700–1712 (2006).
21. Venkataraman, K., Guja, K. E., Garcia-Diaz, M. & Karzai, A. W. Non-stop mRNA decay: a special attribute of trans-translation mediated ribosome rescue. *Front. Microbiol.* **5**, 93 (2014).
22. Karzai, A. W. & Sauer, R. T. Protein factors associated with the SsrA.SmpB tagging and ribosome rescue complex. *Proc. Natl. Acad. Sci. U. S. A.* **98**, 3040–3044 (2001).
23. Chadani, Y. *et al.* Ribosome rescue by Escherichia coli ArfA (YhdL) in the absence of trans-translation system: Ribosome rescue by E. coli ArfA (YhdL). *Mol. Microbiol.* **78**, 796–808 (2010).
24. Chadani, Y., Ito, K., Kutsukake, K. & Abo, T. ArfA recruits release factor 2 to rescue stalled ribosomes by peptidyl-tRNA hydrolysis in Escherichia coli. *Mol. Microbiol.* **86**, 37–50 (2012).

25. Handa, Y., Inaho, N. & Nameki, N. YaeJ is a novel ribosome-associated protein in Escherichia coli that can hydrolyze peptidyl-tRNA on stalled ribosomes. *Nucleic Acids Res.* **39**, 1739–1748 (2011).
26. James, N. R., Brown, A., Gordiyenko, Y. & Ramakrishnan, V. Translational termination without a stop codon. *Science* **354**, 1437–1440 (2016).
27. Huter, P. *et al.* Structural basis for ArfA-RF2-mediated translation termination on mRNAs lacking stop codons. *Nature* **541**, 546–549 (2017).
28. Zeng, F. *et al.* Structural basis of co-translational quality control by ArfA and RF2 bound to ribosome. *Nature* **541**, 554–557 (2017).
29. Ma, C. *et al.* Mechanistic insights into the alternative translation termination by ArfA and RF2. *Nature* **541**, 550–553 (2017).
30. Demo, G. *et al.* Mechanism of ribosome rescue by ArfA and RF2. *eLife* **6**, e23687 (2017).
31. Shimizu, Y. ArfA recruits RF2 into stalled ribosomes. *J. Mol. Biol.* **423**, 624–631 (2012).
32. Zeng, F. & Jin, H. Peptide release promoted by methylated RF2 and ArfA in nonstop translation is achieved by an induced-fit mechanism. *RNA N. Y. N* **22**, 49–60 (2016).
33. Garza-Sánchez, F., Schaub, R. E., Janssen, B. D. & Hayes, C. S. tmRNA regulates synthesis of the ArfA ribosome rescue factor. *Mol. Microbiol.* **80**, 1204–1219 (2011).
34. Chadani, Y. *et al.* trans-translation-mediated tight regulation of the expression of the alternative ribosome-rescue factor ArfA in Escherichia coli. *Genes Genet. Syst.* **86**, 151–163 (2011).

35. Personne, Y. & Parish, T. Mycobacterium tuberculosis possesses an unusual tmRNA rescue system. *Tuberc. Edinb. Scotl.* **94**, 34–42 (2014).

36. Hayes, C. S. & Sauer, R. T. Cleavage of the A Site mRNA Codon during Ribosome Pausing Provides a Mechanism for Translational Quality Control. *Mol. Cell* **12**, 903–911 (2003).

37. Sunohara, T., Jojima, K., Tagami, H., Inada, T. & Aiba, H. Ribosome Stalling during Translation Elongation Induces Cleavage of mRNA Being Translated in Escherichia coli. *J. Biol. Chem.* **279**, 15368–15375 (2004).

38. Garza-Sánchez, F., Gin, J. G. & Hayes, C. S. Amino acid starvation and colicin D treatment induce A-site mRNA cleavage in Escherichia coli. *J. Mol. Biol.* **378**, 505–519 (2008).

39. Subramaniam, A. R., Zid, B. M. & O'Shea, E. K. An integrated approach reveals regulatory controls on bacterial translation elongation. *Cell* **159**, 1200–1211 (2014).

40. Ferrin, M. A. & Subramaniam, A. R. Kinetic modeling predicts a stimulatory role for ribosome collisions at elongation stall sites in bacteria. *eLife* **6**, e23629 (2017).

41. Simms, C. L., Yan, L. L. & Zaher, H. S. Ribosome Collision Is Critical for Quality Control during No-Go Decay. *Mol. Cell* **68**, 361-373.e5 (2017).

42. Juszkiewicz, S. *et al.* ZNF598 Is a Quality Control Sensor of Collided Ribosomes. *Mol. Cell* **72**, 469-481.e7 (2018).

43. Best, K. *et al.* Structural basis for clearing of ribosome collisions by the RQT complex. *Nat. Commun.* **14**, 921 (2023).

44. Matsuo, Y. *et al.* RQT complex dissociates ribosomes collided on endogenous RQC substrate SDD1. *Nat. Struct. Mol. Biol.* **27**, 323–332 (2020).
45. Shen, P. S. *et al.* Protein synthesis. Rqc2p and 60S ribosomal subunits mediate mRNA-independent elongation of nascent chains. *Science* **347**, 75–78 (2015).
46. Kostova, K. K. *et al.* CAT-tailing as a fail-safe mechanism for efficient degradation of stalled nascent polypeptides. *Science* **357**, 414–417 (2017).
47. Shao, S., Brown, A., Santhanam, B. & Hegde, R. S. Structure and assembly pathway of the ribosome quality control complex. *Mol. Cell* **57**, 433–444 (2015).
48. Zurita Rendón, O. *et al.* Vms1p is a release factor for the ribosome-associated quality control complex. *Nat. Commun.* **9**, 2197 (2018).
49. Bengtson, M. H. & Joazeiro, C. A. P. Role of a ribosome-associated E3 ubiquitin ligase in protein quality control. *Nature* **467**, 470–473 (2010).
50. D'Orazio, K. N. *et al.* The endonuclease Cue2 cleaves mRNAs at stalled ribosomes during No Go Decay. *eLife* **8**, e49117 (2019).
51. Shoemaker, C. J., Eyler, D. E. & Green, R. Dom34:Hbs1 promotes subunit dissociation and peptidyl-tRNA drop-off to initiate no-go decay. *Science* **330**, 369–372 (2010).
52. Saito, K. *et al.* Ribosome collisions induce mRNA cleavage and ribosome rescue in bacteria. *Nature* **603**, 503–508 (2022).
53. Fujihara, A. *et al.* Detection of tmRNA-mediated trans-translation products in Bacillus subtilis. *Genes Cells Devoted Mol. Cell. Mech.* **7**, 343–350 (2002).
54. Ito, K. *et al.* Trans-translation mediated by Bacillus subtilis tmRNA. *FEBS Lett.* **516**, 245–252 (2002).

55. Wiegert, T. & Schumann, W. SsrA-mediated tagging in Bacillus subtilis. *J. Bacteriol.* **183**, 3885–3889 (2001).

56. Shimokawa-Chiba, N. *et al.* Release factor-dependent ribosome rescue by BrfA in the Gram-positive bacterium Bacillus subtilis. *Nat. Commun.* **10**, 5397 (2019).

57. Lytvynenko, I. *et al.* Alanine Tails Signal Proteolysis in Bacterial Ribosome-Associated Quality Control. *Cell* **178**, 76-90.e22 (2019).

58. Burroughs, A. M. & Aravind, L. A highly conserved family of domains related to the DNA-glycosylase fold helps predict multiple novel pathways for RNA modifications. *RNA Biol.* **11**, 360–372 (2014).

59. Crowe-McAuliffe, C. *et al.* Structural Basis for Bacterial Ribosome-Associated Quality Control by RqcH and RqcP. *Mol. Cell* **81**, 115-126.e7 (2021).

60. Filbeck, S. *et al.* Mimicry of Canonical Translation Elongation Underlies Alanine Tail Synthesis in RQC. *Mol. Cell* **81**, 104-114.e6 (2021).

61. Takada, H. *et al.* RqcH and RqcP catalyze processive poly-alanine synthesis in a reconstituted ribosome-associated quality control system. *Nucleic Acids Res.* **49**, 8355–8369 (2021).

62. Svetlov, M. S. *et al.* Peptidyl-tRNA hydrolase is the nascent chain release factor in bacterial ribosome-associated quality control. *Mol. Cell* **84**, 715-726.e5 (2024).

63. Cerullo, F. *et al.* Bacterial ribosome collision sensing by a MutS DNA repair ATPase paralogue. *Nature* **603**, 509–514 (2022).

64. Pinto, A. V. *et al.* Suppression of Homologous and Homeologous Recombination by the Bacterial MutS2 Protein. *Mol. Cell* **17**, 113–120 (2005).

65. Roche, E. D. & Sauer, R. T. Identification of Endogenous SsrA-tagged Proteins Reveals Tagging at Positions Corresponding to Stop Codons. *J. Biol. Chem.* **276**, 28509–28515 (2001).

66. Ude, S. *et al.* Translation Elongation Factor EF-P Alleviates Ribosome Stalling at Polyproline Stretches. *Science* **339**, 82–85 (2013).

67. Doerfel, L. K. *et al.* EF-P Is Essential for Rapid Synthesis of Proteins Containing Consecutive Proline Residues. *Science* **339**, 85–88 (2013).

68. Nakatogawa, H. & Ito, K. The Ribosomal Exit Tunnel Functions as a Discriminating Gate. *Cell* **108**, 629–636 (2002).

69. Su, T. *et al.* Structural basis of l-tryptophan-dependent inhibition of release factor 2 by the TnaC arrest peptide. *Nucleic Acids Res.* **49**, 9539–9547 (2021).

70. Gong, F. & Yanofsky, C. Instruction of translating ribosome by nascent peptide. *Science* **297**, 1864–1867 (2002).

71. Bhushan, S. *et al.* SecM-stalled ribosomes adopt an altered geometry at the peptidyl transferase center. *PLoS Biol.* **9**, e1000581 (2011).

72. Polikanov, Y. S., Aleksashin, N. A., Beckert, B. & Wilson, D. N. The Mechanisms of Action of Ribosome-Targeting Peptide Antibiotics. *Front. Mol. Biosci.* **5**, 48 (2018).

73. Wilson, D. N. The A-Z of bacterial translation inhibitors. *Crit. Rev. Biochem. Mol. Biol.* **44**, 393–433 (2009).

74. Buskirk, A. R. & Green, R. Ribosome pausing, arrest and rescue in bacteria and eukaryotes. *Philos. Trans. R. Soc. B Biol. Sci.* **372**, 20160183 (2017).

75. Matsuo, Y. *et al.* Ubiquitination of stalled ribosome triggers ribosome-associated quality control. *Nat. Commun.* **8**, 159 (2017).

76. Filbeck, S., Cerullo, F., Pfeffer, S. & Joazeiro, C. A. P. Ribosome-associated quality-control mechanisms from bacteria to humans. *Mol. Cell* **82**, 1451–1466 (2022).

77. Ikeuchi, K. *et al.* Collided ribosomes form a unique structural interface to induce Hel2-driven quality control pathways. *EMBO J.* **38**, (2019).

78. Koo, B.-M. *et al.* Construction and Analysis of Two Genome-Scale Deletion Libraries for Bacillus subtilis. *Cell Syst.* **4**, 291-305.e7 (2017).

79. Guérout-Fleury, A. M., Frandsen, N. & Stragier, P. Plasmids for ectopic integration in Bacillus subtilis. *Gene* **180**, 57–61 (1996).

80. Guiziou, S. *et al.* A part toolbox to tune genetic expression in Bacillus subtilis. *Nucleic Acids Res.* **44**, 7495–7508 (2016).

81. Zheng, S. Q. *et al.* MotionCor2: anisotropic correction of beam-induced motion for improved cryo-electron microscopy. *Nat. Methods* **14**, 331–332 (2017).

82. Zhang, K. Gctf: Real-time CTF determination and correction. *J. Struct. Biol.* **193**, 1–12 (2016).

83. Zivanov, J. *et al.* New tools for automated high-resolution cryo-EM structure determination in RELION-3. *eLife* **7**, e42166 (2018).

84. Punjani, A., Rubinstein, J. L., Fleet, D. J. & Brubaker, M. A. cryoSPARC: algorithms for rapid unsupervised cryo-EM structure determination. *Nat. Methods* **14**, 290–296 (2017).

85. Jumper, J. *et al.* Highly accurate protein structure prediction with AlphaFold. *Nature* **596**, 583–589 (2021).

86. Goddard, T. D. *et al.* UCSF ChimeraX: Meeting modern challenges in visualization and analysis. *Protein Sci. Publ. Protein Soc.* **27**, 14–25 (2018).

87. Adams, P. D. *et al.* PHENIX: a comprehensive Python-based system for macromolecular structure solution. *Acta Crystallogr. D Biol. Crystallogr.* **66**, 213–221 (2010).

88. Glover, M. L. *et al.* NONU-1 Encodes a Conserved Endonuclease Required for mRNA Translation Surveillance. *Cell Rep.* **30**, 4321-4331.e4 (2020).

89. Lamers, M. H. *et al.* The crystal structure of DNA mismatch repair protein MutS binding to a G x T mismatch. *Nature* **407**, 711–717 (2000).

90. Saxena, S. *et al.* Escherichia coli transcription factor NusG binds to 70S ribosomes. *Mol. Microbiol.* **108**, 495–504 (2018).

91. Zhou, W. *et al.* PPR-SMR protein SOT1 has RNA endonuclease activity. *Proc. Natl. Acad. Sci. U. S. A.* **114**, E1554–E1563 (2017).

92. Chiba, S. & Ito, K. Multisite Ribosomal Stalling: A Unique Mode of Regulatory Nascent Chain Action Revealed for MifM. *Mol. Cell* **47**, 863–872 (2012).

93. Damke, P. P., Dhanaraju, R., Marsin, S., Radicella, J. P. & Rao, D. N. Mutations in the nucleotide binding and hydrolysis domains of Helicobacter pylori MutS2 lead to altered biochemical activities and inactivation of its in vivo function. *BMC Microbiol.* **16**, 14 (2016).

94. Fukui, K. *et al.* Structural and functional insights into the mechanism by which MutS2 recognizes a DNA junction. *Structure* **30**, 973-982.e4 (2022).

95. Trinquier, A., Durand, S., Braun, F. & Condon, C. Regulation of RNA processing and degradation in bacteria. *Biochim. Biophys. Acta BBA - Gene Regul. Mech.* **1863**, 194505 (2020).

96. Mathy, N. *et al.* 5'-to-3' exoribonuclease activity in bacteria: role of RNase J1 in rRNA maturation and 5' stability of mRNA. *Cell* **129**, 681–692 (2007).

97. Fei, X., Bell, T. A., Barkow, S. R., Baker, T. A. & Sauer, R. T. Structural basis of ClpXP recognition and unfolding of ssrA-tagged substrates. *eLife* **9**, e61496 (2020).

98. Burroughs, A. M. & Aravind, L. The Origin and Evolution of Release Factors: Implications for Translation Termination, Ribosome Rescue, and Quality Control Pathways. *Int. J. Mol. Sci.* **20**, 1981 (2019).

99. Safdari, H. A. *et al.* Structure of Escherichia coli heat shock protein Hsp15 in complex with the ribosomal 50S subunit bearing peptidyl-tRNA. *Nucleic Acids Res.* **50**, 12515–12526 (2022).

100. Yan, L. L., Simms, C. L., McLoughlin, F., Vierstra, R. D. & Zaher, H. S. Oxidation and alkylation stresses activate ribosome-quality control. *Nat. Commun.* **10**, 5611 (2019).

101. Sinha, N. K. *et al.* EDF1 coordinates cellular responses to ribosome collisions. *eLife* **9**, e58828 (2020).

102. Wu, C. C.-C., Peterson, A., Zinshteyn, B., Regot, S. & Green, R. Ribosome Collisions Trigger General Stress Responses to Regulate Cell Fate. *Cell* **182**, 404-416.e14 (2020).

103. Moore, S. D. & Sauer, R. T. The tmRNA System for Translational Surveillance and Ribosome Rescue. *Annu. Rev. Biochem.* **76**, 101–124 (2007).

104. Yanofsky, C. Attenuation in the control of expression of bacterial operons. *Nature* **289**, 751–758 (1981).

105. Molodtsov, V., Wang, C., Firlar, E., Kaelber, J. T. & Ebright, R. H. Structural basis of Rho-dependent transcription termination. *Nature* **614**, 367–374 (2023).

106. Wang, C. *et al.* Structural basis of transcription-translation coupling. *Science* **369**, 1359–1365 (2020).

107. Bailey, E. J., Gottesman, M. E. & Gonzalez, R. L. NusG-mediated Coupling of Transcription and Translation Enhances Gene Expression by Suppressing RNA Polymerase Backtracking. *J. Mol. Biol.* **434**, 167330 (2022).

108. Wee, L. M. *et al.* A trailing ribosome speeds up RNA polymerase at the expense of transcript fidelity via force and allostery. *Cell* **186**, 1244-1262.e34 (2023).

109. Johnson, G. E., Lalanne, J.-B., Peters, M. L. & Li, G.-W. Functionally uncoupled transcription–translation in Bacillus subtilis. *Nature* **585**, 124–128 (2020).

110. Gollnick, P., Babitzke, P., Antson, A. & Yanofsky, C. Complexity in regulation of tryptophan biosynthesis in Bacillus subtilis. *Annu. Rev. Genet.* **39**, 47–68 (2005).

111. Babitzke, P. & Yanofsky, C. Reconstitution of Bacillus subtilis trp attenuation in vitro with TRAP, the trp RNA-binding attenuation protein. *Proc. Natl. Acad. Sci. U. S. A.* **90**, 133–137 (1993).